nature communications

Article

https://doi.org/10.1038/s41467-024-54068-6

A single NLR gene confers resistance to leaf and stripe rust in wheat

Received: 11 June 2024

Accepted: 31 October 2024

Published online: 15 November 2024

Check for updates

Davinder Sharma[1,2], Raz Avni[1,2,3], Juan Gutierrez-Gonzalez[4,5], Rakesh Kumar[1,2,16], Hanan Sela[1,6], Manas Ranjan Prusty[1,2], Arava Shatil-Cohen[1], István Molnár[7,17], Kateřina Holušová[7], Mahmoud Said[7,8], Jaroslav Doležel[7], Eitan Millet[1], Sofia Khazan-Kost[1,2], Udi Landau[1], Gerit Bethke[4], Or Sharon[1], Smadar Ezrati[1], Moshe Ronen[1], Oxana Maatuk[1], Tamar Eilam[1], Jacob Manisterski[1], Pnina Ben-Yehuda[1], Yehoshua Anikster[1,18], Oadi Matny[9], Brian J. Steffenson[9], Martin Mascher[3,10], Helen J. Brabham[11,12], Matthew J. Moscou[13], Yong Liang[2], Guotai Yu[14,15], Brande B. H. Wulff[14,15], Gary Muehlbauer[4] ✉, Anna Minz-Dub[1] ✉ & Amir Sharon[1,2] ✉

Nucleotide-binding leucine-rich repeat (NLR) disease resistance genes typically confer resistance against races of a single pathogen. Here, we report that *Yr87/Lr85*, an NLR gene from *Aegilops sharonensis* and *Aegilops longissima*, confers resistance against both *P. striiformis tritici* (*Pst*) and *Puccinia triticina* (*Pt*) that cause stripe and leaf rust, respectively. *Yr87/Lr85* confers resistance against *Pst* and *Pt* in wheat introgression as well as transgenic lines. Comparative analysis of *Yr87/Lr85* and the cloned Triticeae NLR disease resistance genes shows that *Yr87/Lr85* contains two distinct LRR domains and that the gene is only found in *Ae. sharonensis* and *Ae. longissima*. Allele mining and phylogenetic analysis indicate multiple events of *Yr87/Lr85* gene flow between the two species and presence/absence variation explaining the majority of resistance to wheat leaf rust in both species. The confinement of *Yr87/Lr85* to *Ae. sharonensis* and *Ae. longissima* and the resistance in wheat against *Pst* and *Pt* highlight the potential of these species as valuable sources of disease resistance genes for wheat improvement.

Leaf rust (caused by *Puccinia triticina* Eriks., *Pt*) and stripe rust (caused by *P. striiformis* Westend. f. sp. *tritici* Eriks., *Pst*) are common and economically important diseases of cultivated wheat (*Triticum aestivum* L.), capable of destroying entire fields if untreated[1,2]. Apart from chemical fungicides, disease resistance (*R*) genes are the primary means to protect wheat against rust pathogens. Although *R* gene mediated broad-spectrum adult-stage resistance has been observed[3,4], most *R* genes typically confer resistance against a limited set of races of a single pathogen. Therefore, multiple *R* genes are necessary to confer durable resistance against a single pathogen. In recent years, farmers have faced an increase in the incidence of rust diseases and a steady rise in the annual losses that are associated with the appearance of highly aggressive pathogen isolates[5,6], the emergence of pathogen races with altered virulence[1,7], and changes in pathogen distribution as a result of global warming[8]. These factors emphasize the importance of discovering new sources of rust resistance to help protect wheat productivity. Wheat contains over 200 designated rust *R* genes, including approximately 84 each against *Pt* and *Pst* (*Lr1–Lr80* and *Yr1–Yr86*, respectively) and approximately 65 against the stem rust pathogen *P. graminis* Pers.:Pers. f. sp. *tritici* Eriks. and E. Henn. (*Pgt*) (*Sr2–Sr66*)[9,10]. Most of these genes derive from species in the primary gene pool of wheat, such as *Aegilops tauschii* (Coss.) and tetraploid and diploid *Triticum* species that can be readily crossed with modern wheat. Plants within the secondary gene pool, which includes species

A full list of affiliations appears at the end of the paper. ✉e-mail: muehl003@umn.edu; annamin1@tauex.tau.ac.il; amirsh@tauex.tau.ac.il

such as *Aegilops* of the section Sitopsis, have not been extensively exploited. Utilization of this genetic reservoir is restricted owing to the lack of homoeologous recombination, which necessitates the use of a haploid hybrid with homoeologous pairing mutation (*ph1b*), and due to the presence of gametocidal genes that limit interspecies hybridization[11–13]. Recent advancements in gene isolation approaches have led to a marked increase in the cloning of disease resistance genes[14–21]. To date, 32 rust-resistance genes have been cloned, with more than a half in the last five years, and many of these originate from species in the secondary wheat gene pool[22]. Most of the cloned cereal *R* genes are of the nucleotide-binding leucine-rich repeat (NLR) type, each encoding a unique intracellular receptor that recognizes a specific pathogen effector protein[23]. Other types of monocot *R* genes, so far discovered only in Triticeae, include tandem kinase proteins (TKPs), wall-associated kinases (WAKs), and mixed lineage kinase domain-like (MLKL) proteins[24–26]. The advances in gene discovery pipelines along with development of efficient wheat genetic transformation and gene editing protocols[27–29] open the door to more robust exploitation of species in the secondary and tertiary gene pools for wheat improvement.

Aegilops sharonensis Eig and *Ae. longissima* Schweinf. & Muschl. are closely related diploid species of the section Sitopsis (secondary gene pool of wheat) that are rich in traits of agricultural importance[30–35]. Here, we isolate and characterize a leaf and stripe rust resistance gene from these species, expanding our understanding of their genetic defenses. To isolate the gene from *Ae. sharonensis*, we use wheat introgression lines[36,37] and a combination of mutant chromosome purification and sequencing (MutChromSeq), which involves flow sorting and sequencing of mutant chromosomes[38], combined with mutational transcriptomics RNA sequencing (RNA-Seq)[19,24,39]. For *Ae. longissima*, we use the association genetics *R* gene enrichment sequencing (AgRenSeq) pipeline[16], which correlates disease resistant traits with NLR immune receptors, on a diversity panel of 244 accessions. The two systems independently reveal an orthologous NLR gene, which is named *Yr87/Lr85* that is unique to these two *Aegilops* species. Unlike most NLR-type *R* genes, which are specific to a single pathogen, *Yr87/Lr85* confers resistance against two different pathogens, *Pst* and *Pt*. Expressing the *Ae. longissima Yr87/Lr85* in the wheat cv. Fielder confers resistance against otherwise virulent *Pst* and *Pt* races, confirming that *Yr87/Lr85* confers stripe and leaf rust resistance in wheat.

Results

Cloning of the Yr87/Lr85 gene from *Ae. sharonensis*

Leaf and stripe rust-resistance from *Ae. sharonensis* (AEG-548-4) was previously introgressed into wheat cv. Galil[36]. The resistance was mapped to a 17-Mb region on chromosome 6B-6S^{sh} in the D42 introgression line[37] (Fig. 1a). To isolate the candidate resistance gene(s), we used ethyl methanesulfonate (EMS) mutagenesis on 3086 seeds of the D42 line, which yielded 1158 M_2 families. Following stepwise screening with *Pt* #526-24 and *Pst* #5006 isolates that are avirulent on the D42 parental line, we identified 16 independent M_3 lines that were susceptible to both isolates (Supplementary Fig. 1). We confirmed the presence of the introgressed segment in all 16 M_3 lines by diagnostic PCR[37] (Supplementary Fig. 2). The F_2 progeny of crosses made between a homozygous *Pt/Pst* susceptible individual and a homozygous *Pt/Pst* resistant M_3 individual resulted in monogenic (1 susceptible to 3 resistant) segregation (Supplementary Table 1), and crosses made between a homozygous *Pt/Pst* susceptible individual and the recurrent wheat parent cv. Galil produced uniformly susceptible progenies, collectively indicating that the resistance to both pathogens is conferred by a single genetic locus.

To isolate the gene, we took a mutational transcriptomics approach[19,24,39], using five EMS-mutant lines (Supplementary Table 2), their progenitor D42 line, and the *R* gene donor *Ae. sharonensis* AEG-548-4. We inoculated the plants with the *Pt* #526-24 and *Pst* #5006 isolates and extracted RNA from leaf samples at 0 hours post-inoculation (hpi), 24 hpi, and 48 hpi. Following RNA sequencing and processing, we searched the data for candidate genes that are expressed in both D42 and AEG-548-4 at one or more time points and contained EMS-derived mutations in at least three of the five mutant lines. The analysis yielded several putative candidates, the most promising being transcript TRINITY_DN6116_c0_g1 (Supplementary Data 1 and 2). This transcript was expressed at all time points, contained mutations in all five mutant lines (one of the lines carried two mutations), and encoded a putative protein with a nucleotide-binding site (NBS) and leucine-rich repeat (LRR) domains. All the single nucleotide polymorphisms (SNPs) in the mutant lines were within the same coding sequence (CDS) and resulted in an amino acid substitution (Fig. 1a and Supplementary Table 3). To analyze the non-coding regions, we performed chromosome sorting and sequencing and obtained high-quality chromosome enrichment and sequences for the mutant lines. Mapping of the reads to a D42 assembly that was sequenced at a high depth (Supplementary Table 4) revealed three genomic contigs that spanned the entire sequence of the candidate gene (Supplementary Data 3).

To validate the function of the candidate gene, we used virus induced gene silencing (VIGS)[40] to suppress its expression in the D42 line by targeting two non-overlapping gene-specific sequences (Fig. 1a and Supplementary Data 4). The VIGS plants showed >75% reduced expression of the candidate gene (Fig. 1b) and were susceptible to the *Pt* #526-24 and *Pst* #5006 isolates (Fig. 1c), confirming that the gene is required for leaf rust and stripe rust resistance. We temporarily designated the candidate gene *Yr87/Lr85*.

To visualize the YR87/LR85 protein, we generated a three-dimensional model of its predicted structure (Fig. 1d). The predicted YR87/LR85 protein exhibits a structural resemblance to coiled-coil (CC) NLRs. This includes the presence of a conventional NBS domain and an unusually elongated (36 repeats) horseshoe-like configuration C-terminal LRR domain. For comparison, the typical LRR repeats in previously cloned NLR resistance genes vary within the range of 6–31 and an average number of ~24 repeats (Supplementary Fig. 3a). Further analysis revealed that the exceptionally long LRR repeat consists of two predicted horseshoe structures that are separated by a short spacer sequence. All the amino acid substitutions found in the EMS mutants mapped to functional domains within the predicted YR87/LR85 protein (Fig. 1a, d and Supplementary Table 3). Two of the mutations were in externally facing parts of the LRR domain (Supplementary Fig. 3b), which is a diversification hotspot that possibly facilitates pathogen recognition[41,42]. Two EMS lines had a mutation in the first LRR domain, resulting in the loss of resistance to both the *Pt* and *Pst* isolates. This finding suggests that the LRR domain may confer resistance to different pathogens.

Cloning of the Yr87/Lr85 gene from *Ae. longissima*

To search for additional rust-resistance genes, we screened a diversity panel of 244 *Ae. longissima* accessions by inoculation of seedlings separately with two *Pt* isolates, #12460 and #12337 (see methods for details). We obtained similar results with these isolates, with a resistance frequency of 30% in the *Ae. longissima* panel (Fig. 2a). To identify candidate leaf rust-resistance genes, we followed the AgRenSeq pipeline using the pan-cereal NLR capture library Tv_3[15,16] and the phenotyping results of the plants infected with the two *Pt* isolates. We generated de novo assemblies from the Illumina short-read sequences from all 244 accessions, filtered the sequences using NLR-Parser, and performed *k*-mer-based association genetics analysis with 137 accessions exhibiting observable traits.

We found an association between resistance to both isolates and the presence of two contigs, 71,128 and 71,798 (Supplementary Data 5),

https://doi.org/10.1038/s41467-024-54068-6

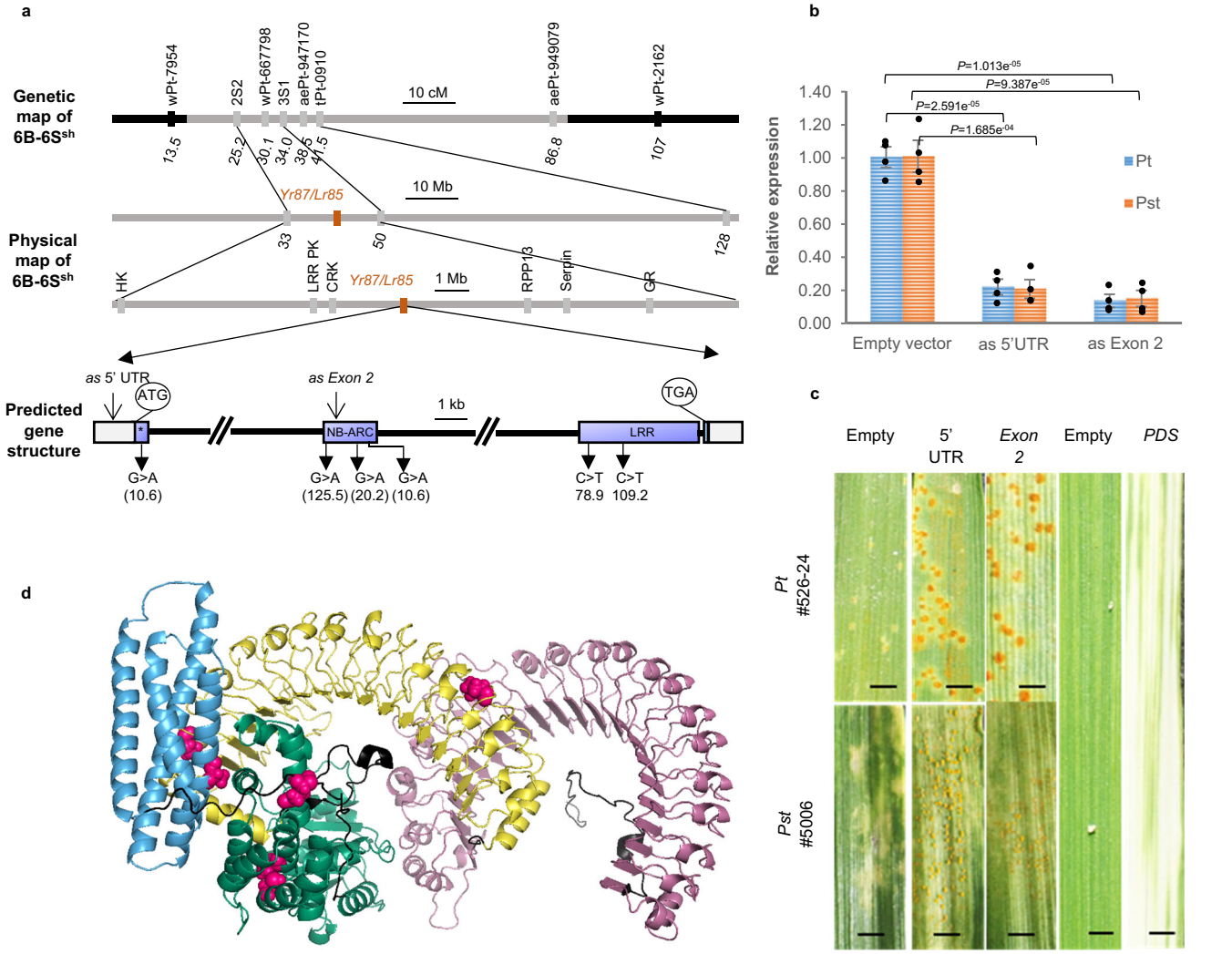

Fig. 1 | Cloning and functional validation of *Ae. sharonensis Yr87/Lr85*. **a** Genetic (cM) and physical (Mb) maps of the *Yr/Lr* locus in the D42 introgression line[36,37]: black, wheat background; gray, *Aegilops* background; genes in the interval delimiting the presence of *Yr87/Lr85*: HK histidine kinase; LRR PK LRR protein kinase, CRK cysteine-rich receptor kinase, RPP13 disease resistance protein RPP13, Serpin serine protease inhibitors, GR glutamate receptor. Predicted gene structure and protein domains according to NLRscape: black lines denote introns, shaded rectangles denote untranslated regions (UTRs), lilac rectangles are exons, closed arrows denote EMS point mutations, open arrows denote locations of sequences targeted by VIGS (for details see Supplementary Data 4), double slash denotes aproximately 3kb of intronic region not shown, asterisk denotes the Rx-CC domain. The number below the nucleotide in parentheses represents the mutant lines. The number below the nucleotide in parentheses represents the mutant line numbers. **b** *Yr87/Lr85* expression levels in D42 following VIGS. Data are mean ± s.e.m. Significant differences were evaluated using a two-tailed Student's *t*-test. $n = 4$ biological replicates. Black dots represent individual data points. *P* values are shown on the graph. **c** Reaction of D42 to leaf and stripe rust isolates after VIGS targeting the 5′ UTR and exon 2 of *Yr87/Lr85*. Wheat *Phytoene deacetylase* (*PDS*) was used as a control to monitor the effectiveness of gene silencing. Scale bars, 2 mm. **d** AlphaFold2 predicted YR87/LR85 protein structure, where the Rx-CC (blue) and NB-ARC (green) domains mostly comprise α-helixes and the LRR (yellow and pink) domains comprise a β-helical "horseshoe" structures. Magenta spheres denote EMS point mutations. Source data are provided as a Source Data file.

that were localized to an unmapped region in the reference genome ("chromosome unknown"). To precisely map the *R* gene, we re-sequenced the *Ae. longissima* AEG-6782-2 reference line using PacBio and generated an improved genome assembly (Supplementary Fig. 4)[43,44] with a contig N50 of 16 Mb. Using Hi-C data, the assembly was ordered into 7 pseudomolecules that make up 5.9 Gb (98.6% of the assembled sequence) and contain 67.8 kb gaps, whereas the first assembly, which was based on short-read data, had 931.4 Mb gaps. The improved assembly enabled us to map the two AgRenSeq NLR candidate contigs to an open reading frame on chromosome 6S at position 51,756,423–51,772,629 (16,207 bp) (Fig. 2b). Surprisingly, sequence alignments of the candidate *Ae. longissima* leaf rust-resistance gene and *Ae. sharonensis Yr87/Lr85* revealed that the two genes were almost identical (Supplementary Data 6): they were exactly the same size (16,207 bp), contained three highly similar introns, and had nearly identical exons that differed only in three synonymous nucleotide substitutions and produced a 4533-bp CDS (Supplementary Data 7) with a predicted protein of 1510 amino acids. Hence, we independently isolated an orthologous rust-resistance gene from *Ae. sharonensis* and *Ae. longissima* using two different approaches.

To verify the function of *Yr87/Lr85* from *Ae. longissima* in resistance to *Pst* and *Pt*, we produced transgenic wheat lines (cv. Fielder) expressing *Ae. longissima Yr87/Lr85* cDNA or a synthetic genomic DNA (gDNA) clone that included the four exons separated by shortened introns, both with the native promoter and termination sequences (see Methods and Fig. 2c and Supplementary Fig. 5 for details). We generated independent primary transgenic events (T_0), selected three events each with various copy numbers of either the cDNA or the synthetic gDNA clone (Supplementary Table 5), produced homozygous T_1 and T_2 progenies, and tested their response to infection with

https://doi.org/10.1038/s41467-024-54068-6

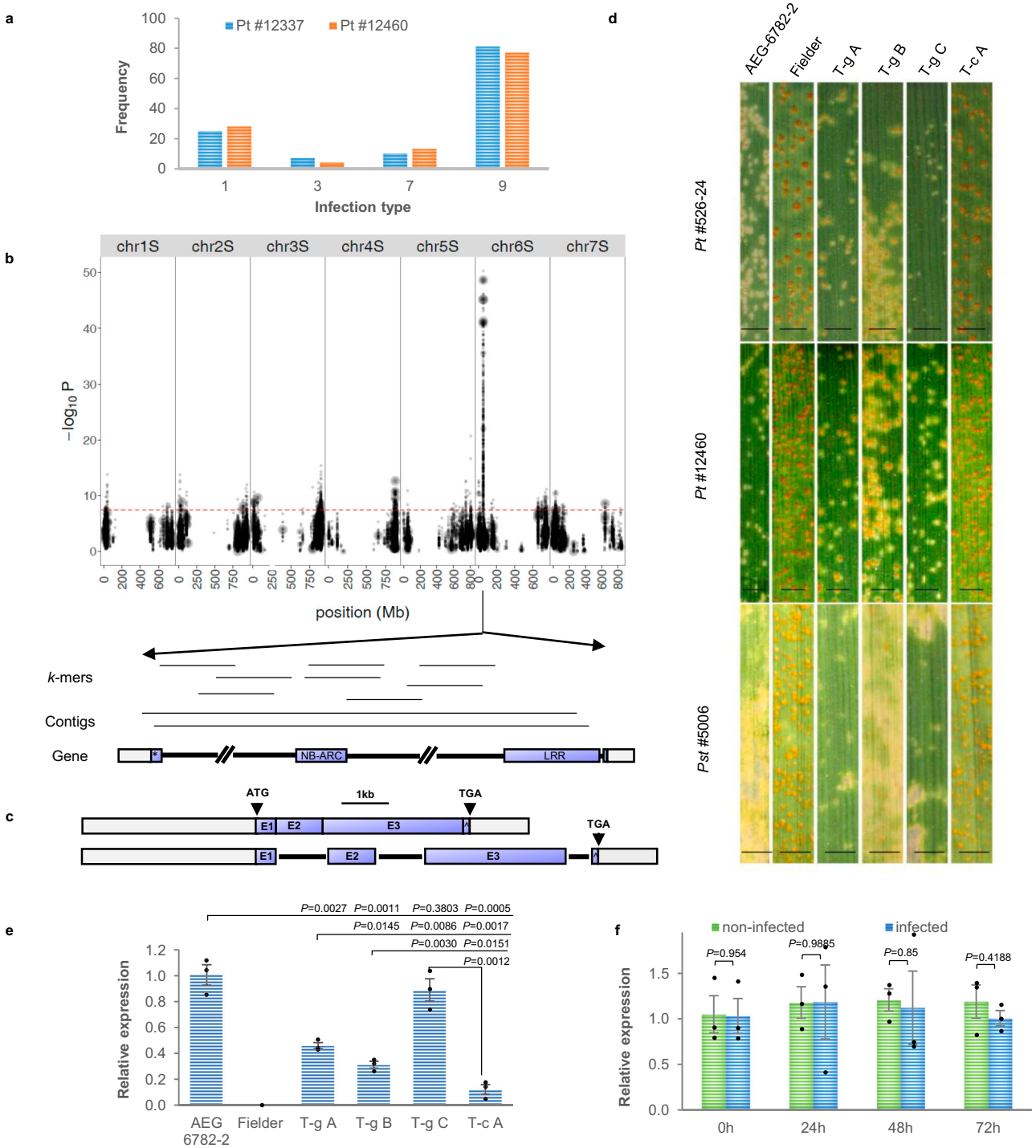

Fig. 2 | Cloning and functional validation of *Ae. longissima Yr87/Lr85*. **a** Distribution of leaf rust resistance across 137 *Ae. longissima* accessions. Infection types range from 1 (complete resistance) to 9 (fully susceptible). Pearson's correlation coefficient was calculated to assess the relationship between infection types of the two isolates, revealing a strong correlation ($r = 0.91$, $P = 5.97e^{-53}$). A two-tailed test was used, and no adjustments were made for multiple comparisons. **b** Identification of *Yr87/Lr85* using *Pt* isolate #12337. The *x*-axis shows the genomic position on the AEG-6782-2 genome assembly, the *y*-axis represents the score of the *k*-mers associated with resistance across the diversity panel. The association score is defined as the negative log of the *P* value obtained using the general linear model (GLM). The dotted red line is the significance threshold at $P = 0.001$ and is adjusted for multiple comparisons using "Bonferroni' correction,* denotes Rx-CC domain. **c** Diagrams of the gene constructs used to transform wheat cv. Fielder. Shaded rectangles denote promoter and terminator regions, lilac rectangles denote exons, black lines (bottom scheme) denote partial (first and second introns, where 4 kb and 5.5 kb were excluded respectively from the construct) or full (third) intron sequences, ^ denotes Exon 4. **d** Reaction of exemplary transgenic lines to infection with *Pt* and *Pst* isolates. gDNA (T-g) and cDNA (T-c) transgenic lines. Scale bars, 2 mm. **e** Relative transcript levels of the *Yr87/Lr85* gene in gDNA (T-g) and cDNA (T-c) transgenic lines vs. wild-type Fielder and in *Ae. longissima* AEG-6782-2 at the seedling stage. **f** Relative transcript levels of the *Yr87/Lr85* gene in uninfected (green) or post-infected (blue) leaves, at the seedling stage, after infection with *Pt* isolate #12460. Data are mean ± s.e.m. Significant differences were evaluated using a two-tailed Student's *t*-test. $n = 3$ biological replicates. Black dots represent individual data points. *P* values are shown on the graph. The D6 protein kinase (*D6PK*) like gene (XM_044524929) was used as an internal control. Source data are provided as a Source Data file.

the *Pt* and *Pst* isolates. The three cDNA transgenic lines were all susceptible to the *Pt* (#526-24 and #12460) and *Pst* (#5006) isolates, whereas the three gDNA transgenic lines showed variable degrees of resistance (Fig. 2d). Reverse transcription-quantitative PCR (RT-qPCR) analysis revealed that *Yr87/Lr85* expression levels in the cDNA transgenic plants were at least 2.5-fold lower than those in the gDNA plants and ~6-fold lower than that in *Ae. longissima* (Fig. 2e). The relatively low gene expression levels in the tested cDNA transgenic lines (Fig. 2e) suggested that the introns within the coding sequence are important for proper *Yr87/Lr85* gene expression[45]. Furthermore, expression of the *Yr87/Lr85* gene did not differ between infected and uninfected plants (Fig. 2f), and the resistance level conferred by *Yr87/Lr85* was not compromised at relatively high temperatures (28 °C day/22 °C night; Supplementary Fig. 6). We also tested two additional transgenic lines with two additional isolates of both *Pt* (TNBJS and MNPSD) and *Pst* (v-37 and v-40) from North America (USA) and found high levels of resistance (Supplementary Fig. 7). To check if *Yr87/Lr85* provides resistance to other pathogens, we inoculated the transgenic Fielder plants with two isolates of *Pgt* (stem rust #2135 and #2127) and three isolates of *Blumeria graminis* f. sp. *tritici* (*Bgt*; powdery mildew, #15, #70 and #101) pathogens. All isolates were virulent (Supplementary Fig. 8) indicating that *Yr87/Lr85* confers specific resistance to *Pst* and *Pt*.

Yr87/Lr85 confers quantitative resistance in seedlings and adult plants

To gain insight into the mode of resistance conferred by *Yr87/Lr85*, we inoculated wild type and *Yr87/Lr85*-transgenic Fielder plants with the *Pt* and *Pst* isolates and then stained the leaf samples with FITC-labeled wheat germ agglutinin (WGA), which specifically stains fungal cell walls[46]. The *Pt* and *Pst* isolates penetrated and grew within leaf tissues of the resistant plants, but fungal development was drastically reduced, and the area occupied by the fungi was substantially larger in the susceptible cv. Fielder (Fig. 3a–c). Similar results were obtained with susceptible and resistant accessions of *Ae. longissima* (Supplementary Fig. 9). The resistance response was similar in seedlings and in adult plants (Fig. 3a), and this common phenotype was paralleled by a similar expression level of the *Yr87/Lr85* gene in young and adult plants (Supplementary Fig. 10a). Finally, the *Yr87/Lr85* gene was expressed in most tissues except roots (Supplementary Fig. 10b).

Staining of reactive oxygen species (ROS) with diamino benzidine (DAB) showed that the transgenic plants accumulated lower levels of

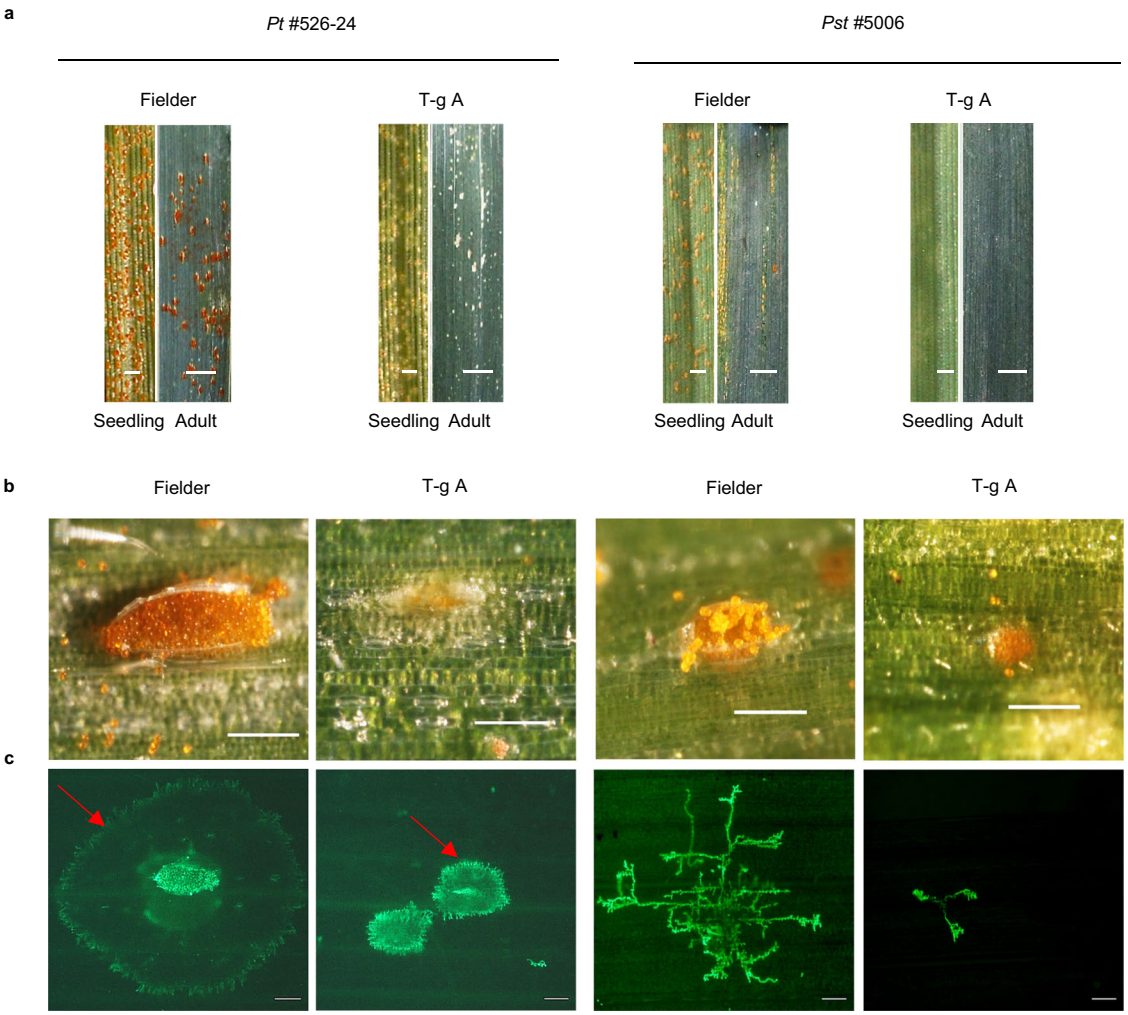

Fig. 3 | *Yr87/Lr85* confers resistance in seedlings and adult plants. a Pustule development on seedling (*Pt*, 7 days post-inoculation [dpi]; *Pst*, 14 dpi) and adult (*Pt*, 18–20 dpi; *Pst*, 17–20 dpi) leaves of wheat cv. Fielder and transgenic plants expressing *Ae. longissima Yr87/Lr85*. Scale bars, 2 mm. Light (**b**) and fluorescent (**c**) micrographs of leaf segments of wheat seedlings inoculated with *Pt* or *Pst*. **b** *Yr87/Lr85* transgenic seedlings developed chlorotic halos that occasionally produced micropustules (*Pt*, 7 dpi; *Pst*, 14 dpi). Scale bars, 200 μm. **c** Leaves were stained with WGA-FITC. Spores of *Pt* and *Pst* germinated and penetrated the epidermis of *Yr87/Lr85* transgenic plants but progressed slower and developed smaller colonies within the leaf compared with infection of cv. Fielder plants. The arrows mark the edges of the colonies. Scale bars, 200 μm. The experiments were independently repeated three times, yielding consistent results.

ROS than wild type Fielder plants, however the DAB staining occupied a larger space, suggesting a quantitative defense response (Supplementary Fig. 11). We concluded that *Yr87/Lr85* hinders infection to *Pst* and *Pt* by slowing down pathogen development (Fig. 3b, c and Supplementary Fig. 9), and although it does not completely block fungal growth, it prevents disease development in seedlings and mature plants.

Yr87/Lr85 is only found in *Ae. sharonensis* and *Ae. longissima*

We searched for *Yr87/Lr85* orthologs in other species. A local BLAST search of the v2.0 *Ae. longissima* assembly (AEG-6782-2) using the *Yr87/Lr85* CDS as a query revealed a single copy of *Yr87/Lr85* in the *Ae. longissima* genome, while the published *Ae. sharonensis* genome[24] did not contain *Yr87/Lr85* homologs. To understand the relationship of *Yr87/Lr85* relative to known NLR encoding genes, we performed a large-scale phylogenetic analysis using the NBS domain of NLRs from *Ae. tauschii*, *Brachypodium distachyon*, *Hordeum vulgare* (barley), *Oryza sativa* (rice), *Setaria italica* (Foxtail millet), *Sorghum bicolor*, *T. aestivum* (wheat), *T. urartu*, and *Zea mays* (maize) based on the approach of Bailey et al.[47]. YR87/LR85 was located in the C24 clade within a subclade that does not include known resistance genes (Supplementary Fig. 12a). The rice PI5-1/PI5-2 and PII-1/PII-2 resistance genes are in a sister subclade to YR87/LR85[48]. Phylogenetic analysis using full-length NLRs in the YR87/LR85 subclade only found species from the Bambusoideae, Oryzoideae, and Pooideae (BOP) clades (Supplementary Fig. 12b). The orthogroup including YR87/LR85 found four NLRs: YR87/LR85, *Ae. tauschii* EMT11349 (*RGA1*, Resistance Gene Analog 1), barley HORVU.MOREX.r3.3HG0316460.1, and *T. urartu* TRIUR315482P1 (Supplementary Fig. 12b). A global BLAST search of the NCBI and cereals-specific databases using the *Yr87/Lr85* CDS as a query revealed sequence similarity in plant species from three tribes: Triticeae, Poeae, and Brachypodieae (Supplementary Data 8). We further searched the genomes of hexaploid wheat[20,49,50] and the wheat D genome progenitor *Ae. tauschii*[51,52] for *Yr87/Lr85* homologs (Supplementary Table 6). The two genes with the highest sequence similarity to *Yr87/Lr85* were the *Ae. tauschii* putative disease resistance gene *RGA1*, which is 87% identical to the predicted *Yr87/Lr85* CDS, and the *T. urartu RGA2-like* putative disease resistance gene, with 83% nucleotide identity. All other predicted genes shared less than 80% sequence identity and/or had less than 80% coverage. Interestingly, a global BLAST search using the YR87/LR85 predicted protein sequence as a query showed only 79% identity to *Ae. tauschii* RGA1, and the rest of the sequences had less than 65% identity (Supplementary Data 9). Collectively, this shows that *Yr87/Lr85* belongs to a large clade of NLRs from BOP species and has putative orthologs in only three species in the Triticeae.

To check whether *Ae. tauschii RGA1* is a functional homolog of *Yr87/Lr85*, we examined the response to the *Pt* #526-24 isolate of 15 *Ae. tauschii* accessions, eight that harbor *RGA1* and seven that lack *RGA1*. There was no correlation between resistance of the accessions to *Pt* #526-24 and the presence of *RGA1* (Supplementary Table 7). To further examine if *RGA1* is a functional homolog of *Yr87/Lr85*, we used VIGS to suppress expression of the *RGA1* gene (Supplementary Data 4) in the *Ae. tauschii* accession AEG-9907-0. *RGA1* silenced plants did not exhibit any variation in response to *Pt* #526-24 when compared to plants inoculated with the empty vector, further suggesting that the *Ae. tauschii RGA1* is not a functional homolog of the *Yr87/Lr85* gene (Supplementary Fig. 13).

A phylogenetic analysis using the predicted full-length YR87/LR85 protein sequence or just the LRR and NBS domains and the protein sequences of previously cloned NLR genes[9], showed that the predicted YR87/LR85 protein is most closely related to the wheat TSN1 ToxA sensitivity protein (Supplementary Fig. 14 and Supplementary Data 10). However, we found only low sequence similarities when using the CC domain as a query, indicating that this domain differs from that in previously cloned NLRs. Structural homology analysis of the predicted structure of the YR87/LR85 protein using the FoldSeek database showed partial structural similarities to several predicted NLR-type resistance proteins (Supplementary Fig. 15), however all candidates lacked homology in the C-terminal part of the proteins and this analysis did not reveal new functional or phylogenetic information. Based on the above analyses, we conclude that we could not identify a functional homolog of the *Ae. sharonensis* and *Ae. longissima Yr87/Lr85* gene in current databases.

Ae. sharonensis grows in a narrow stretch (>15 km wide) along the eastern coast of the Mediterranean, overlapping with *Ae. longissima*, which is more widespread and can be found more inland and to the south[53]. To fully classify the allelic diversity of *Yr87/Lr85* in *Ae. sharonensis* and *Ae. longissima*, we used iterative de novo assembly and *k*-mer fingerprinting on RenSeq data from diverse collections of *Ae. sharonensis* ($N = 204$) and *Ae. longissima* ($N = 244$). *Yr87/Lr85* exists as a presence/absence variation with the gene present in 36% of *Ae. sharonensis* accessions (73/204) and 21% of the *Ae. longissima* accessions (52/244) (Supplementary Data 11). Multiple alleles exist based on variation in the open reading frame (*Ae. sharonensis*, 19 alleles; *Ae. longissima*, 18 alleles) and amino acid sequence (*Ae. sharonensis*, 17 variants; *Ae. longissima*, 15 variants). The majority of alleles were unique to an individual species, where 44% of them were found in a single genotype, and only four alleles were shared between *Ae. sharonensis* and *Ae. longissima*. In total, 24% of the genotypes contained alleles that were shared with the other species (Supplementary Table 8). Several alleles carry interrupted open reading frames including AEG-2172 (AGSH008), AEG-7888 (AGSH010), AEG-2229 (AGSH054), AEG-2704 (AGSH057), and AEG-4844 (AGSH060). Interestingly, while the *Yr87/Lr85* allele AEG-401 [AGSH039] is shared between *Ae. sharonensis* and *Ae. longissima*, it appears to be non-functional as it carries an insertion in the second exon that may impact gene expression (Supplementary Data 12).

Classification of alleles based on sequence identity to YR87/LR85 revealed that the majority of resistance to wheat leaf rust in *Ae. sharonensis* and *Ae. longissima* can be explained by YR87/LR85 (Fig. 4a and b). In *Ae. longissima*, of 35 accessions predicted to carry a functional *Yr87/Lr85* (allele that confers resistance in transgenic lines described above), 31 accessions (88.5%) were resistant (IT 1-3) and four were susceptible (IT 7-9) to *Pt* isolate #12460 (Supplementary Data 12). Of 166 accessions predicted to carry a non-functional or deletion of *Yr87/Lr85*, 22 accessions were resistant (IT 1-3), two accessions had intermediate scores (IT 5), and 142 were susceptible (IT 7-9). In *Ae. sharonensis*, of 44 accessions predicted to carry a functional *Yr87/Lr85* allele, only 28 accessions (63%) were resistant (IT 1-3) and 16 were susceptible (IT 7-9) to *Pt* isolate THBJ[35,54] (Supplementary Data 13). Of 100 accessions predicted to carry a non-functional or deletion of *Yr87/Lr85*, 31 accessions were resistant (IT 1-3), three accessions had intermediate scores (IT 5), and 66 were susceptible (IT 7-9). Little sequence variation was observed between alleles with intact open reading frames, with a maximum of four amino acid differences relative to functional alleles.

Recombination analysis did not find any recombination events between the *Yr87/Lr85* CDS alleles. The inferred maximum likelihood (ML) phylogenetic tree of the alleles (Fig. 4c) revealed no clear separation between the *Ae. sharonensis* and the *Ae. longissima* alleles. None of the higher order branches were specific to one species. Moreover, no clear-cut geographic pattern was observable, except for one branch stemming from the root at the bottom of the tree that originated from the north. Additionally, in 18% of the alleles, accessions with the same allele were found more than 75 km apart, and in 75% of the collection sites with more than one accession, there were two to four different alleles. This pattern suggests that there were several horizontal gene transfer events between the two species and that there

https://doi.org/10.1038/s41467-024-54068-6

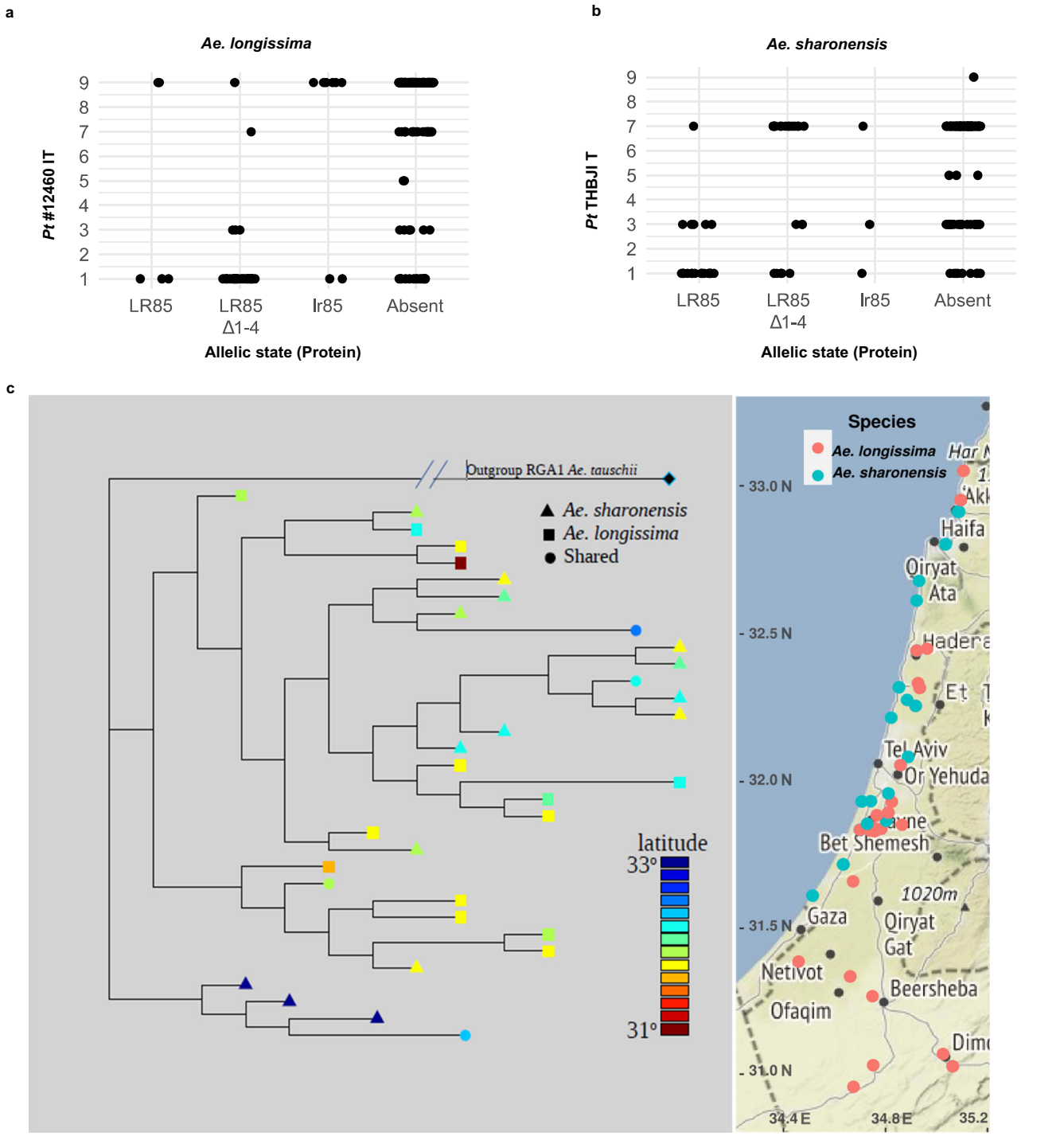

Fig. 4 | *Yr87/Lr85* accounts for the majority of resistance to *P. triticina* in *Ae. sharonensis* and *Ae. longissima* populations and underwent horizontal gene transfer. a Phenotype by allele analysis of *Ae. longissima* accessions carrying identical LR85, from one to four amino acid variations (LR85 Δ1-4), interrupted open reading frame or large InDel (*lr85*), and absence of *Lr85*. **b** Phenotype by allele analysis of *Ae. sharonensis* accessions carrying identical LR85, from one to four amino acid variations (LR85 Δ1-4), interrupted open reading frame or large InDel (*lr85*), and absence of *Lr85* with *P. triticina* isolate THBJ infection type (IT), phenotypic data from Olivera et al.[35,54]. **c** ML tree based on alleles' sequences, color – average latitude of the origin of accessions that have the allele, shape-species. Map shows distribution of the *Ae. sharonesis* (blue) and *Ae. longissima* (red) samples used.

is likely evolutionary pressure to maintain diversity of the gene within populations.

Discussion

Multiple disease resistance is usually conferred by non-NLR *R* genes with a general function, such as the rice (*Oryza sativa*) broad-spectrum resistance genes *Pi21* and *Ptr* that encode a proline-rich protein[55] and a protein with four Armadillo repeats[56], respectively. Other examples are the wheat pleiotropic-effect *R* genes *Lr34* that encodes an ABC transporter[57] and *Lr67* that encodes a hexose transporter[58]. Though rare, resistance conferred by a single NLR *R* gene against taxonomically distant pathogens has been reported. The *RESISTANT TO RALSTONIA*

SOLANACEARUM 1 (*RRS1*) and *RESISTANT TO P. SYRINGAE 4* (*RPS4*) NLR genes in Arabidopsis (*Arabidopsis thaliana*) function cooperatively to confer resistance against three bacterial pathogens, *Pseudomonas syringae*, *Ralstonia solanacearum*, and *Xanthomonas campestris*, and one fungal pathogen, *Colletotrichum higginsianum*[59]. Likewise, the *Mi* NLR gene in tomato (*Solanum lycopersicum*) confers resistance to three types of pests: root knot nematode (*Meloidogyne* spp.), potato aphid (*Macrosiphum euphorbiae*), and whitefly (*Bemisia argentifoli*)[60–62]. Recognition of XOPQ1 (*Roq1*) confers resistance in *Nicotiana benthamiana* to the phytopathogenic bacteria *Xanthomonas* and *Pseudomonas*[63,64].

In grasses, the only examples of multiple-resistance NLR genes are the barley (*Hordeum vulgare*) *Mildew locus a* (*Mla*) genes *Mla3*, *Mla7*, and *Mla8*. All three genes confer resistance to the host-adapted powdery mildew pathogen *B. graminis* f. sp. *hordei*, and in addition, each gene confers resistance against major pathogens of other crops: *Mla3* confers resistance to the rice blast pathogen *Pyricularia oryzae* (syn. *Magnaporthe oryzae*) by specifically recognizing the Pwl2 effector protein[65], and *Mla7* and *Mla8* confer resistance against the wheat stripe rust pathogen *Pst*[66,67]. In wheat, it has been reported that *Sr15/Lr20* and *Lr16/Sr23* confer resistance to stem and stripe rust pathogens, however, the genes have not been isolated and their molecular nature is unknown[68]. Marais et al.[69] introgressed a leaf and stripe rust-resistance locus from *Ae. sharonensis* into chromosome 6A of bread wheat; however, the resistance was associated with two separate genes, *Lr56* and *Yr38*, that segregated between the offspring, and it is unrelated to *Yr87/Lr85*, which is also located on chromosome 6. Hence, the *Yr87/Lr85* reported here is a rare case, particularly in wheat, of a cloned NLR gene that confers resistance to two distinct wheat pathogens.

Yr87/Lr85 did not prevent host invasion and did not completely block the pathogens, but it slowed pathogen growth and prevented disease progression. In this respect, it is more similar to adult plant resistance or slow rusting, which are manifested only in adult plants, unlike complete resistance, which is usually observed at seedling stage[70–72]. However, the *Yr87/Lr85* gene conferred equally effective resistance in seedlings as well as in adult plants, hence it should be considered an all stage resistance (ASR) gene. *Yr87/Lr85* resistance is specific against leaf and stripe rust as it was found ineffective against stem rust or powdery mildew pathogens, hence it is not as broad as that of *Lr34/Yr18/Sr57/Pm38, Lr46/Yr29/Sr58/Pm39* and *Lr67/Yr46/Sr55/Pm46*, which confer resistance against all four pathogen species. The resistance conferred by *Yr87/Lr85* was effective against all the *Pst* and *Pt* isolates that we have tested, including highly virulent races, indicating its high potential in breeding programs.

The *Yr87/Lr85* phenotype resembles the resistance that is conferred by the *Sr21* and *Sr13* stem rust-resistance genes, which also slow pathogen development. *Sr21* and *Sr13* confer only partial resistance to stem rust, are more effective at high temperatures[73–75] and in the case of *Sr21* but not *Sr13*, the resistance level is correlated with gene expression level. The expression of both genes leads to upregulation of a set of pathogen-responsive genes at high temperatures, suggesting that they share common pathways and mechanisms. The expression of *Yr87/Lr85* is constitutive and stable, is unaffected by the presence of the pathogens, plant age, or temperature, and the resistance it provides is equally successful in both seedlings and adult plants, suggesting a distinct mechanism compared to *Sr21* and *Sr13*.

How *Yr87/Lr85* confers resistance against two different pathogen species is unclear. Assuming that, as in other cases, resistance is triggered by recognition of a fungal effector, the YR87/LR85 protein possibly recognizes two different protein effectors, as in the case of *N. benthamiana* ROQ1 that recognizes different effectors from different bacterial species[76]. Along this line, we can rule out a differential role of the two LRR domains since mutations in one of them abolished resistance against both *Pst* and *Pt*. Alternatively, the different pathogen species may contain a common effector; this is the case for the wheat *Tsn1* gene that confers sensitivity to the ToxA effector from three different necrotrophic fungal pathogens, *Parastagonospora nodorum*, *Pyrenophora tritici-repentis* and *Bipolaris sorokiniana* that cause the diseases septoria nodorum blotch, tan spot, and spot blotch, respectively[77]. Since the *Yr87/Lr85* gene sequence is almost identical in *Ae. sharonensis* and *Ae. longissima*, both possibilities are currently viable.

The phylogenetic analysis showed that *Yr87/Lr85* belongs to an expanded clade of NLRs in the BOP and the functional haplotype was only found in *Ae. sharonensis* and *Ae. longissima*. Sequence variation in the promoter, terminator, introns, or untranslated regions likely explains the lack of full predictive power of YR87/LR85 for resistance to *Pt* as suggested by the allele analysis. The homolog with the highest sequence similarity, an uncharacterized *RGA1* gene with 87% nucleotide and 79% amino acid identity to *Yr87/Lr85*, was found in *Ae. tauschii* (Supplementary Data 8 and 9), the donor of the hexaploid wheat D subgenome and a member of the same clade as *Ae. sharonensis* and *Ae. longissima*[78]. All other predicted genes in recently published genomic data, including the D genome wheat species, various *Ae. tauschii* accessions, and the wheat ABD genome species[45–50], showed less than 80% sequence similarity to *Yr87/Lr85* (Supplementary Table 6). The presence or absence of RGA1 in various accessions of *Ae. tauschii*, or silencing of *RGA1* in the *Ae. tauschii* resistant accession AEG-9907-0, did not have any impact on response to the *Pt* #526-24 isolate. Therefore, *RGA1* does not seem to be a functional homologue of *Yr87/Lr85*.

Ae. sharonensis and *Ae. longissima* are closely related, with a mean identity of 98.6% for all high-confidence genes[78]. However, the mean identity of NLR genes between the two species is only 87%, suggesting that each species contains a significant number of unique *R* genes. Phylogenetic analysis of the NLRs from the different genomes highlighted groups of genes or specific targets for further study; for example, the two branches that lacked cloned *R* genes and clades rich in cloned genes that might indicate an evolutionary hotspot[78]. We expect that the availability of *Ae. sharonensis* and *Ae. longissima* high quality diversity panels and robust genome resources, coupled with powerful long read sequencing pipelines such as PacBio[79] and whole-genome *k*-mer-based association mapping[17], will enable researchers to systematically explore and rapidly mine these unique genetic resources to improve wheat and other cereal crops.

Methods

Plant and pathogen materials

The *Aegilops sharonensis*, *Ae. longissima*, *Ae. tauschii* accessions (AEG accessions) and cv. Galil (*Triticum aestivum* L.)[36,37,78] were obtained from the Harold and Adele Lieberman Germplasm Bank in the Institute for Cereal Crops Research (ICCR) at Tel Aviv University (https://en-lifesci.tau.ac.il/icci). Seeds of the recombinant and transgenic lines generated in the current study have been deposited in the same germplasm bank. *Ae. tauschii* [17]accessions were obtained from the Department of Agronomy and Plant Genetics, University of Minnesota, St. Paul, Minnesota. The *Ae. sharonensis* diversity panel consisting of 193 accessions, including AEG-548-4 (TH548)[36,37], originated from 24 collection sites spanning the whole *Ae. sharonensis* geographic distribution in Israel. The *Ae. longissima* diversity panel consisting of 380 accessions, including AEG-6782-2[78], originated from 80 collection sites spanning the whole *Ae. longissima* geographic distribution in Israel. All accessions were self-fertilized for three to five generations, with bagged heads to prevent cross-fertilization. Accessions were selected to maximize their geographic distribution and minimize the number of accessions originating from the same collection site. Wheat cv. Fielder (NSGC cltr. 17268) was obtained from the National Small Grains Germplasm Research Facility, USDA-ARS- United States (NSGC).

Puccinia triticina Eriks. (*Pt*, leaf rust) isolates #526-24 (race MFBKG)[80] #12460 (race MCDTB), and #12337 (race MFPPB), *P.*

striiformis Westend. f. sp. *tritici* Eriks. (*Pst*, stripe rust) isolate #5006 (virulence/avirulence (V/Av) formula Yr6,7,8,9,11,12,17,19,sk,18,A/Yr1,5,10,15,24,26,sp)[36] and *P. graminis* Pers.:Pers. f. sp. *tritici* Eriks. and E. Henn. (*Pgt*, stem rust) isolates #2135 (race TTTTC)[81] and #2127 (race TTTTF) were from the stocks of the ICCR. *Pt* races TNBJS and MNPSD were from James Kolmer at the Cereal Disease Lab, United States, and *Pst* isolates PsTv-40 (V/Av formula 6,7,8,9,10,24,27,32,43,44,Tr1,Exp2/1,5,15,17,SP,Tye) and PsTv-37 (V/Av formula 6,7,8,9,17,27,43,44,Tr1,Exp2/1,5,10,15,24,32,SP,Tye)[82] were from Xianming Chen's lab at Washington State University. *Blumeria graminis* f. sp. *tritici* (*Bgt*, powdery mildew) isolates #15, #70 and #101[83] were from the Department of Vegetables and Field Crops, Institute of Plant Sciences, ARO-Volcani Center and Haifa University. The *P. triticina* and *P. graminis* nomenclature is according to the updated code for North American differential hosts for *P. triticina*, USDA.

Plant inoculation and phenotyping

Seedlings were tested and selected for leaf rust and stripe rust resistance[84]. Briefly, plants were sown and grown in small pots in a temperature-controlled greenhouse at 22 ± 2 °C with a 14-h day/10-h night photoperiod. Inoculation was performed with a suspension of urediniospores in lightweight mineral oil (Soltrol 170), and the oil on the inoculated plants was allowed to evaporate. Routinely, seedlings were inoculated at one- (7–10 days after planting, for leaf rust) or two-leaf stage (10–12 days after planting, for stripe rust), adult plants were inoculated at early grain filling (Zadoks growth stage 75)[85]. For gene expression studies, plants were inoculated by brushing leaves with fresh spores. For the VIGS assay, the plants were inoculated 13 days after transfection with Barley Stripe Mosaic Virus (BSMV). Following inoculation, for all applications, plants were incubated for 24 h in a dew chamber (100% relative humidity) and then transferred to the greenhouse. For leaf rust inoculation, plants were incubated for 24 h in a dew chamber at 18 °C and grown in the greenhouse for 12–14 days at 22 °C. For the high-temperature assay, plants were initially infected with *Pt* (leaf rust) isolates, incubated in a dew chamber for 24 h, and then moved to a growth chamber for 12–14 days at 25 °C. For stripe rust inoculation, plants are maintained in a dew chamber for 24 h (12 h at 9 °C in the dark, followed by 12 h at 15 °C in the light) and then transferred to a growth chamber for 14–17 days at 15 °C. For stepwise infection with both leaf and stripe rust, plants were first inoculated with leaf rust, incubated in a dew chamber for 24 h, then for 4–6 days in the greenhouse, and then inoculated with stripe rust and incubated in a dew chamber and growth chamber as described above. For all types of inoculations, three replicates for each accession were tested, and plants were scored for infection type (IT) 7–10 dpi for *Pt* and 14 dpi for *Pst*, on a standard 0 to 4 or 0 to 9 scale[84]. ITs were converted from a 0–4 scale to a 1–9 scale for convenience, where values of 0–2 (converted to 1–3 on the new scale) were considered a resistance response and values of 3–4 (converted to 7–9 on the new scale) were considered a susceptible response.

Mutagenesis and screening for susceptible *Ae. sharonensis Yr87/Lr85* introgression lines

Homozygous resistant introgression line D42, containing a segment (including *Yr87/Lr85*) derived from *Ae. sharonensis* accession AEG-548-4 in the hexaploid bread wheat cultivar Galil background (RY32-3-14[36]), was selected and 3086 seeds were treated with EMS (Sigma–Aldrich)[14]. Briefly, dry seeds were treated for 16 h with 200 mL of 0.5% EMS solution while being rolled on an orbital shaker (TS-400, MRC) to ensure maximum exposure of the seeds to EMS. The excess solution was then removed, the seeds were washed with 500 mL tap water three times, each for 1 h, and then planted in 0.8-L pots. M_1 seeds were grown in the greenhouse with controlled conditions of 14-h light and 23 °C/18 °C day/night temperature, and seeds of M_2 families (single heads) were collected. Ten seeds per family were phenotyped sequentially with *P. triticina* isolate #526-24 and *P. striiformis* isolate #5006. M_3 seeds derived from susceptible M_2 plants were also phenotyped with the above-mentioned rust isolates to confirm that M_2 susceptible plants were true mutants. DNA of all susceptible M_3 mutants was validated for the presence of the introgressed segment containing the resistance gene *Yr87/Lr85* by PCR amplification[37].

Flow cytometric sorting and sequencing

Susceptible mutants derived from independent M_4 families and the D42 parental line were selected for MutChromSeq[14]. Briefly, root tip meristem cells were synchronized using hydroxyurea, paused in metaphase using amiprophos-methyl, and mildly fixed in formaldehyde. Intact chromosomes were released by mechanically homogenizing 100 root tips in 600 µL ice-cold IB buffer[86]. Prior to flow cytometric analysis, chromosomes were labeled by fluorescence in situ hybridization in suspension (FISHIS) using 5′-FITC-$(GAA)_7$-FITC-3′ and 5′-FITC-$(ACG)_7$-FITC-3′ oligonucleotide probes (Integrated DNA Technologies, Inc., Iowa, USA)[87] and chromosomal DNA was stained by 4′,6-diamidino 2-phenylindole (DAPI) at 2 µg/mL. Chromosome analysis and sorting were performed using a FACSAria II SORP flow cytometer and sorter (Becton Dickinson Immunocytometry Systems, San José, USA). Chromosome samples were analyzed at rates of 900–1400 particles per second. Bivariate flow karyotypes FITC pulse area (FITC-A) vs. DAPI pulse area (DAPI-A) fluorescence were acquired and 20,000 events were recorded to create a bivariate flow karyotype for each sample. Sort regions delimiting populations of chromosome 6B-6S^{sh} were set on flow karyotypes and chromosomes were sorted at a rate of 12–24 particles per second. Two batches of 25,000–76,000 copies of chromosome 6B-6S^{sh} were sorted from each sample into PCR tubes containing 40 µL sterile deionized water (Supplementary Fig. 16). Chromosome contents of flow-sorted fractions were estimated by microscopic observation of 1500–2000 chromosomes sorted into a 6-µL drop of primed in situ DNA labeling (PRINS) buffer containing 2.5% sucrose onto a microscope slide. Air-dried chromosomes were labeled by FISH with probes for the pSc119.2 repeat, Afa family repeat, and 45S rDNA[88]. At least 100 chromosomes were classified following the karyotype[89,90], to determine the chromosome content of the flow-sorted samples and to assign the populations observed on bivariate flow karyotypes to particular chromosomes. Flow-sorted chromosome samples were treated with proteinase K, and their DNA was purified and amplified by multiple displacement amplification using an Illustra GenomiPhi V2 DNA Amplification Kit (GE Healthcare, Chicago, IL, USA)[91]. Purities in 6B-6S^{sh} chromosome fractions and total DNA amount prepared from the flow-sorted chromosome fractions are listed in Supplementary Table 2. Libraries for sequencing were prepared using NEBNext Ultra II DNA Library Prep Kit for Illumina (New England BioLabs, Massachusetts, USA) and sequenced on HiSeq2500 (Illumina, San Diego, CA, USA) using Hiseq Rapid SBS Kit v2. 2x250 bp (Illumina, San Diego, CA, USA), and paired-end reads were produced. Each mutant library was sequenced on one lane of a HiSeq2500 with 150-bp paired-end reads (for each of the mutants) and 250-bp paired-end reads at 70× coverage for wheat parental line D42.

MutCromSeq data analysis

The quality of sequenced raw fastq libraries was checked with Fastqc[92] (http://www.bioinformatics.babraham.ac.uk/projects/fastqc). Overall, reads from parental line D42 and EMS mutants were of good quality, and no trimming was required. The MutCromSeq protocol[38] was applied to the high-quality filtered reads with few modifications. For de novo assembly of the parental D42 introgression line, three assemblers were tested: the commercial CLC and the two open software MaSuRCA v.3.4.2[93] (https://github.com/alekseyzimin/masurca) and Abbys v.2.0.2[94], all with default parameters. Assembly contiguity statistics were calculated with abyss-fac from the Abbys suite. RepeatMasker v.4.0.5 (www.repeatmasker.org) with the TriticeaeRepeat Database

(TREP)[95] was used to mask repetitive sequences in the de novo assemblies. To align sequenced reads and generate pileup files for each mutant and the wild type, BWA v.0.7.17[96] with the Aln algorithm was used. The forward and reverse aligned reads were combined with the Sampe algorithm into the corresponding SAM format files, which were converted to BAM files, sorted, filtered for duplicates, and used to generate pileup files with SAMtools v.1.9[97]. To lessen the impact of contaminations, we selected reads aligned with a mapping quality (-q) of 30 or above. The java programs Pileup2XML.jar and Mut transcriptomics.jar, part of the Mut transcriptomics pipeline[38] were used to filter the pileup files. First, Pileup2XML.jar was used to screen pileup files for single nucleotide variations (SNV), with the parameters -a and -c set to 0.2 and 7, for the maximum reference allele frequency and minimum coverage allowed, respectively. Second, Mut transcriptomics.jar with -c 7 -a 0.01 -z 2 -n 5 or 3 was used to combine the individual XML output files from the previous step and call candidate contigs. The z parameter controls the maximum number of mutants that are allowed to have a mutation at the same position, and n establishes the minimum number of mutants that need to have a mutation in a contig to be reported as a candidate. Finally, the IGV browser[98] (https://software.broadinstitute.org/software/igv/) was used to visually inspect candidate contigs for validation. Both Gmap[99] with --min-trimmed-coverage=0.90 --min-identity=0.90, and BLASTn, with *e*-value threshold of 1E-50, from the ncbi_blast+ suite[100] were used to map contigs to chromosome $6S^{sh}$ of the *Ae. sharonensis* assembly[24] and chromosome 6B of the wheat cv. Chinese Spring reference genome assembly (IWGSC_RefSeq_v1.0)[101].

Genomic DNA and RNA isolation, gene expression, and copy number analysis

For most applications, gDNA was extracted from leaves by the modified CTAB method[102]. Briefly, 0.1 g of frozen leaves was ground to a fine powder using two steel beads, on a GenoGrinder 2010 (cat. no. 20-101-15; Fischer Scientific), the sample was then mixed with 1 mL of CTAB buffer (2% CTAB, 20 mM EDTA, 100 mM Tris-HCl pH 8.0, 1.4 M NaCl, 0.5% sodium disulfite, 0.1% β-mercaptoethanol) and incubated at 65 °C for 45 min. After incubation, a mixture of chloroform:isoamylalcohol (24:1) was added, mixed and the sample was subjected to centrifugation at 15,000 *g* for 10 min. Supernatant was transferred to a new centrifuge tube, 3 µL of RNase A (10 mg/mL) were added and followed by incubation at 37 °C for 30 min. Then an equal volume of chloroform:isoamylalcohol (24:1) mixture was added and the samples were subjected to centrifugation at 15,000 *g* for 10 min. The upper phase was transferred to a new tube and samples were mixed with 0.6 volume of ice-cold isopropanol, incubated at −20 °C for 60 min and centrifuged at 15,000 *g* at 4 °C for 10 min. The supernatant was discarded, and the pellet was washed twice with ice-cold 70% ethanol and dried. The DNA was then dissolved in 100 µl of ultra-pure water. For PacBio genome sequencing, a modification of the CTAB method incorporating polyvinylpolypyrrolidone and sucrose was used. Briefly, ~3.5 g of frozen leaf tissue was ground to a fine powder, using mortar and pestle in liquid nitrogen. The sample was then mixed with 13 mL of a pre-heated (65 °C) DNA isolation buffer that was prepared by combining three solutions in a 1:1:0.4 ratio, consisting of Solution A (0.35 M sorbitol, 0.1 M Tris-HCl pH 7.5, 5 mM EDTA), Solution B (0.2 M Tris-HCl pH 7.5, 0.05 M EDTA, 2 M NaCl, 2% CTAB), and Solution C (5% N-lauroylsarcosine sodium salt), with the addition of 1% polyvinylpolypyrrolidone (PVPP) and 0.3% natrium disulfite to the final mixture. The sample was incubated at 65 °C for 90 min. After incubation, an equal volume of chloroform:isoamylalcohol (24:1) mixture was added, gently mixed for 10 min and the sample was subjected to centrifugation at 1600 *g* at 4 °C for 15 min. The upper phase was transferred to a new centrifuge tube and the chloroform extraction was repeated twice. DNA was precipitated by adding 2/3 volume of isopropanol to the supernatant, followed by gentle inversion and incubation at −20 °C for 10 min. The DNA was collected using a Pasteur pipette, washed with 15 mL of 70% ethanol, and incubated overnight at 4 °C. After discarding the ethanol, the DNA was air-dried for 10 min and dissolved in 300 µL of ultra-pure water with heating at 65 °C for 5 min. 10 µL of RNase A (10 mg/mL) was added and the sample was incubated at 37 °C for 30 min. The solution was then mixed with 1 mL of chloroform:isoamyl alcohol (24:1) for 10 min, centrifuged at 1600 *g* at 4 °C for 10 min, and the supernatant was transferred to a new tube. DNA was re-precipitated by adding 1/10 volume of 3 M sodium acetate and 2/3 volume of isopropanol, incubated at −20 °C for 20 min, and centrifuged at 15,000 *g* at 4 °C for 15 min. The DNA was finally dissolved in 500 µl of ultra-pure water. Total RNA was extracted using the DSGT (Dodecyl Sulfate and Guanidine Thiocyanate) extraction method for next-generation sequencing quality RNA[103]. First-strand cDNA was synthesized using the RevertAid First Strand cDNA Synthesis Kit (cat. no. K1622; ThermoFisher). All cDNA samples were diluted fourfold with ultra-pure water prior to use in qPCR. Primers for qPCR were designed to anneal to different exons flanked by introns with amplicon lengths between 140 bp and 170 bp. Each reaction was run with at least three independent biological replicates. qPCR analysis was performed with qPCRBIO SyGreen Mix (PCR Biosystems) on a PikoReal 96 Real-time PCR instrument (Thermo Scientific). The qPCR data were analyzed by the comparative $2^{-\Delta\Delta Ct}$ method[104]. The *D6PK*-like gene (*T. aestivum* protein kinase, XM_044524929) was used as an internal control. Significant differences were analyzed by two-tailed Student's *t*-test. To measure *Yr87/Lr85* expression in *Ae. longissima* accession AEG-6782-2 and in the Galil × *Ae. sharonensis* introgression line D42, 2-week-old seedlings were inoculated with *Pt* #526-24 and *Pst* #5006 isolates. Single leaves from four individual plants were harvested for each treatment at the time of inoculation (T_0) and at 24 hpi, 48 hpi, and 72 hpi. To determine the efficiency of VIGS, fourth leaves of BSMV-infected D42 plants were collected at 7–14 dpi with the rust isolates. To determine the level of gene expression at different growth stages of transgenic Fielder plants, leaves were harvested at seedling, booting, and milk development stage.

The transgene copy number was measured using Droplet PCR[105]. Briefly, gDNA was extracted from 4-week-old T_0 seedlings via the CTAB method as described above, digested with 20 U of *Hae*III enzyme (NEB) in a 50-µL reaction volume at 37 °C for 16 h, and used as a template. Droplet digital PCR (ddPCR) was performed via probe chemistry in a duplex assay for the reference gene *PUROINDOLINE-b* (*PINb*)[106,107] and the target gene bialaphos resistance (*Bar*) gene. Bar Probe1 (Supplementary Data 14) was labeled with HEX at the 5′ end, Iowa Black Hole Quencher at the 3′ end, and with an internal ZEN quencher 9 nucleotides away from the 5′ end. PINb Probe2 (Supplementary Data 14) was labeled with FAM at the 5′ end, Iowa Black Hole Quencher at the 3′ end, and with an internal ZEN quencher 9 nucleotides away from the 5′ end. Primers F12-R12 and F13-R13 were used for *Bar* and *PINb*, respectively (Supplementary Data 14). ddPCR reaction mixes were prepared following the instructions in the ddPCR Supermix for Probes (No dUTP) #1863024 kit (Bio-Rad). Droplets were generated with a QX200 droplet generator (Bio-Rad), and the PCR was run in a C1000 (Bio-Rad) deep-well thermal cycler. The fluorescence of the droplets was measured with a QX200 droplet analyzer (Bio-Rad), and the results were evaluated with the Bio-Rad Quantasoft Pro Software.

Mutational transcriptomics data analysis

The 150-bp paired-end libraries were sequenced by Novogene on an Illumina Novaseq, producing ~40 million reads per sample. Two transcriptomes were used: a combined de novo-assembled transcriptome with the parent D42[24] and the mutant lines; and a reference-guided transcriptome extracted from the AEG-548-4 annotation whose chromosome fragment was introgressed into the D42 genome. For all sequenced libraries, raw fastq reads from 0 hpi, 24 hpi, and 48 hpi were quality filtered with Trimmomatic v.0.33[108] and quality-checked with Fastqc[109] before and after filtering. Trimmomatic was instructed to cut

bases off the start and the end of a read if below a threshold quality of 20 and if the average quality within a window of 4 nucleotides fell below the threshold of 20. For de novo assembly, high-quality reads were pooled and de novo-assembled with Trinity v.2.10.0 using default parameters except to also include super-transcripts. To calculate expression values at 0 hpi, 24 hpi, and 48 hpi, reads were first mapped back to the transcriptome assembly using bowtie2 v.2.3.4.1[110] and samtools v.1.9[97]. RNA from D42 and the EMS-mutant D42 lines (mut_78, mut_109.2, mut_125.5, mut_10.6, and mut_20.2) was extracted and sequenced at three time points (0 hpi, 24 hpi, and 48 hpi), except for line mut_20.2 that was only extracted at 0 hpi and 24 hpi. For the reference-based transcriptome, AEG-548-4 reads from 0 hpi, 24 hpi, and 48 hpi were aligned to the *Ae. sharonensis* chr6S[24] assembly using Star v2.7.1[111] and the annotation file. For both transcriptomes, transcript quantification and Trimmed Mean of M values (TMM) cross-normalization were computed with the RNA-Seq by Expectation Maximization method v.1.3.0[112]. Statistical analyses were conducted in R[113]. The BLASTx program of the BLAST+ tools[100] was used to search and functionally annotate the transcriptomes against the Uniprot-Viridiplantae database[114]. The −e value parameter was set to 1 × E-20 and -max_target_seqs to 1, to report only the top alignment, with otherwise default parameters.

To aid in identifying functional resistance genes, the NLR-Annotator tool[115] was used to annotate the intracellular immune repertoire. The NLR-Annotator pipeline is divided into three steps: (1) dissection of genomic input sequence into overlapping fragments; (2) NLR-Parser, which creates an xml-based interface file; and (3) NLR-Annotator, which uses the xml file as input, annotates NLR loci, and generates output files based on coordinates and orientation of the initial input genomic sequence. The pipeline was run on the de novo-assembled genomic scaffolds and de novo-assembled pooled transcripts, as well as on the AEG-548-4 annotated transcripts, using the MEME suite v.5.0.1.1[116] and otherwise default configuration.

Phylogenetic analysis

The maximum likelihood phylogenetic tree based on NBS domains of NLRs from grasses was constructed according to Bailey et al.[47]. Briefly, NB domains were trimmed and aligned using HMMer (v3.1b2) hmmalign using the HMM profile[47] and parameters “trim” and “amino”. Full length NLRs in the YR87/LR85 clade were aligned using kalign (v3.3) using default parameters. Both trees were constructed using RAxML (v8.2.11) using the JTT substitution model. Bootstrapping was performed using 1000 bootstraps. Using BLASTp (protein–protein BLAST), the YR87/LR85 predicted amino acid sequence was searched for sequence similarities in the monocot taxonomy. BLAST was performed on a database of non-redundant protein sequences and the obtained results were filtered with a percentage identity of 60–90%.

Structural analysis and three-dimensional modeling

The secondary protein structure of YR87/LR85 was predicted using NLRScape (https://nlrscape.biochim.ro/)[117], and the number of LRR repeats was analyzed using LRR predictor (https://lrrpredictor.biochim.ro/)[117]. The 3D structure was predicted using Phyre2 (http://www.sbg.bio.ic.ac.uk/~phyre2/)[53,118] and the AlphaFold2 (v2.3.1)[119] inference pipeline using an NVIDIA A100 GPU processor using the monomer model and max template date of July 26th, 2023. Visualization was performed using ChimeraX (v1.7.1) and PyMol (v2.5.2). Structural homologs search was performed using FoldSeek (https://search.foldseek.com/search)[120].

Phenotyping, sequencing, and association genetics of the *Ae. longissima* diversity panel

Genotyping-by-sequencing data[53] and phenotypic disease resistance data[84] of the collection were used to select 244 genotypically and phenotypically diverse accessions using Core Hunter R package[121] for the AgRenSeq experiment (Supplementary Fig. 17). To filter genes representing the NLR repertoire, the extracted DNA was subjected to NLR capture using a pan-cereal NLR oligo array Tv_3 (Arbor Biosciences, Michigan, USA)[16], and the captured DNA was sequenced on an Illumina HiSeq with 150-bp paired-end reads (Novogene, China). Then, 36 genotypes were selected and sequenced with 250-bp paired-end reads to use as references in AgRenSeq. To assemble contigs of these 36 samples, BFC was used for error correction, $k = 128$ was selected (based on the kmergenie (http://kmergenie.bx.psu.edu/) estimate), and the contigs were assembled using minia (https://github.com/GATB/minia). Association genetics was then used to identify candidate rust-resistance genes[16].

Allele mining

An iterative process of de novo assembly and *k*-mer fingerprinting were used to define the allelic variation in *Ae. sharonensis* and *Ae. longissima*. Initially, genomic data for AEG-546 was used to define the exon regions carrying the open reading frame of *Yr87/Lr85*. De novo assembly was performed with minia (v3.2.5) using default parameters. *k*-mer fingerprinting was performed using the k-mer analysis toolkit (KAT) ‘sect’ command using *Yr87/Lr85* exonic coding sequence as a template and raw RenSeq data as input with default parameters. This process was repeated when an accession was not fully classified based on previously established diversity. The mined alleles were aligned using MUSCLE[122] and the resulting multiple alignment was subjected to recombination detection using recombination detection program RDP[123]. Maximum likelihood (ML) phylogenetic tree as implemented in RDP was inferred from the multiple alignment and plotted with indication of species and geographic locations of the tree tips using in house R script.

Preparation of recombinant DNA fragments and plasmid constructs

The binary vector pRC3646 (Wisconsin Crop Innovation Center, Madison,WI, USA) that contains the *Bar* selectable marker gene was used as the backbone for plasmid construction. Two genomic fragments, 3831 bp upstream of the start codon and 1413 bp downstream of the stop codon of *Yr87/Lr85*, were PCR-amplified from gDNA of the *Ae. longissima* resistant accession AEG-6782-2. Due to the large size of introns (>12 kb), four fragments that contained no more than 1.0 kb of each intron were generated to express a genomic clone (Supplementary Fig. 5). Four different fragments containing the exons and 5′ and 3′ short regions of the flanking introns were amplified. These four DNA fragments were ligated and cloned into a *Bsa*I-digested *pUDP* vector using the NEB Golden Gate Assembly Kit (BsmBI-v2) and transformed into DH5α competent *Escherichia coli* cells. PCR amplification of the cloned gDNA fragment produced a 6490 bp DNA fragment containing the four exons, two shortened introns, and the intact third intron. Next, the gene fragment was combined with the 5′ UTR and promoter (3831 bp) and 3′ UTR and terminator (1413 bp) fragments using Gibson NEBuilder HiFi DNA Assembly Cloning Kit (New England Biolabs), cloned into the *Bsa*I-digested pRC3646 vector, and transformed into NEB STable Competent *E. coli* cells. The cDNA construct was similarly produced but used the full-length *Yr87/Lr85* CDS. Both plasmids were fully sequenced before transfer to *Agrobacterium tumefaciens* strain AGL-1 for wheat transformation; details of primers (F1-R1-F7-R7) are listed in Supplementary Data 14.

VIGS

The BSMV vectors (pα, pβ, pγ:null, and pγ:TaPDS) utilized for gene silencing were based on the corresponding constructs[124]. The pγ vector is modified to contain a ligation-independent cloning (LIC) site to permit direct cloning of the VIGS target sequences. The pγ:TaPDS vector (pγ with the *T. aestivum* phytoene desaturase (*PDS*) gene fragment) was used as a positive control, and the pγ:null vector without

insert was used as a negative control. To identify targets with minimal or no homology to off-target genes, the *Yr87/Lr85* sequence was analyzed using si-Fi (siRNA Finder; http://labtools.ipk-gatersleben.de/) against the entire wheat cDNA annotation IWGSC RefSeq v1.0 (http://plants.ensembl.org/Triticum_aestivum/Info/Index). Two regions (5′ UTR, 243 bp = VIGS1; exon 2, 188 bp = VIGS2) were selected as VIGS target sequences. Target sequences were produced via reverse transcription PCR (RT-PCR) using total RNA extracted from healthy *Ae. longissima* AEG-6782-2 leaves. The pγ vector was linearized with restriction enzyme *Apa*I (New England Biolabs, R0114S) at 25 °C for 2 h to produce a LIC cloning site. Both the linearized pγ vector and purified PCR product were then treated with T4 DNA polymerase (New England Biolabs) to generate the complementary sticky ends. The treated PCR products were mixed with 2 μL treated pγ vector to allow ligation. The mixture was transformed into competent DH5α *E. coli* cells. Plasmids were purified from PCR-verified bacteria and Sanger-sequenced. The verified plasmids were introduced into *A. tumefaciens* strain GV3101 by electroporation and plated on LB agar containing kanamycin (50 μg/mL) and rifampicin (25 μg/mL). Single colonies were propagated overnight, diluted 1:50, and grown at 30 °C overnight. Cultures were spun down and cells were re-suspended in infiltration medium (10 mM MES, 10 mM $MgCl_2$, 200 μM acetosyringone), adjusted to a final optical density of 1.0 at 600 nm, and incubated at room temperature without shaking for 3 h or longer. Equal volumes of *A. tumefaciens* strains carrying either the pγ:VIGS1, pγ:VIGS2, pγ:TaPDS, or pγ:null construct, pα and pβ were combined and infiltrated into the adaxial side of 4-week-old *Nicotiana benthamiana* leaves using a 1-mL syringe. The infiltrated *N. benthamiana* leaves were harvested 6 days post-agroinfiltration and ground using a pre-chilled mortar and pestle in 10 mM potassium phosphate buffer (pH 7.0) containing 1–2% (w/v) Celite 545 AW (Sigma–Aldrich) abrasive. The extracted sap was then used to rub-inoculate the second leaf of two-leaf stage wheat seedlings. Plants were inoculated with rust isolates 13 days after virus infection, and symptoms were recorded after 7 days and 14 days for leaf and stripe rust, respectively.

Transformation and evaluation of rust resistance in transgenic wheat seedlings

Final confirmation of *Yr87/Lr85* activity was performed by generation of transgenic wheat lines using *Agrobacterium tumefacience*-mediated transformation of immature embryos of wheat cv. Fielder[28] with the *Yr87/Lr85* constructs, and testing the response of the transgenic plants to leaf and stripe rust isolates. The validated binary vectors pRC3646:Lr_cDNA or pRC3646:Lr_gDNA were co-transformed with pVS1-VIR (Addgene[125]) into *A. tumefaciens* strain AGL-1 using the heat-shock method. The AGL-1 strains were verified to contain a binary vector harboring the candidate gene and the pVS1-VIR helper plasmid by PCR. The transformed plants were screened by PCR using primers against the *Bar* and *Yr87/Lr85* genes (F8-R8 and F9-R9, respectively, Supplementary Data 14), by RT-PCR using primers against the *Yr87/Lr85* and *D6PK*-like genes (F10-R10 and F11-R11, respectively, Supplementary Data 14), and by spraying with a Basta (glufosinate ammonium). The T_1 plants expressing the *Yr87/Lr85* gene were infected with spores of the leaf rust isolates #12460 and #526-24 to assess the resistance level as described above in "Plant inoculation and phenotyping".

Microscopy

To visualize the infection area, the infected leaves were detached at 2 dpi and 14 dpi and stained with WGA-FITC (L4895-10MG; Sigma)[75] with minor modifications. Leaves were cut into 2-cm pieces and placed in a 10-mL centrifuge tube with 5 mL 1 M KOH and 0.05% Silwet L-77. After 12 h, the KOH solution was gently poured off and the leaves were washed with 10 mL of 50 mM Tris (pH 7.5). This solution was then replaced with another 10 mL of 50 mM Tris (pH 7.5). After 20 min, the Tris solution was removed and replaced with 5 mL 20 μg/mL WGA-FITC. The tissue was stained for 15 min and then washed with 50 mM Tris (pH 7.5). The WGA-FITC-stained tissue was examined under blue light excitation with an Axio Zoom V.16 (Zeiss). The staining of Hydrogen Peroxide was performed using DAB[126].

Genome assembly

Ae. longissima libraries were sequenced by Novogene (https://en.novogene.com) on a PacBio Sequel II[127] using six SMRT cells[43,128]. A SMRTbell library was generated by fragmenting gDNA to appropriate sizes. The DNA fragments were damage-repaired, end-repaired, and A-tailed. The SMRTbell library was produced by ligating universal hairpin adapters onto double-stranded DNA fragments. After the exonuclease and AMPure PB beads purification steps, the sequencing primer was annealed to the SMRTbell templates, followed by binding of the sequencing polymerase to the annealed templates. The software SMRTlink was used to filter and process original sequencing results with the minLength 0 and minReadScore 0.8 parameters. The HiFi read assembly was done using hifiasm (https://github.com/chhylp123/hifiasm; version 0.14) with default parameters. The pseudomolecules were constructed using the TRITEX pipeline[129].

Reporting summary

Further information on research design is available in the Nature Portfolio Reporting Summary linked to this article.

Data availability

The raw Chrom-Seq and RNA-seq data used for MutChromSeq, AgRenSeq, and PacBio reads used for de novo whole-genome assemblies were deposited in the European Nucleotide Archive (ENA) under project numbers PRJEB64238, PRJEB64239, and PRJEB58051, respectively. The *Yr87/Lr85* gene and transcript sequences have been deposited to NCBI under accession PP897794. Seeds of *Ae. longissima* accession AEG-6782-2 [https://www.genesys-pgr.org/a/70e40670-d268-4260-b249-99599de7a833] and *Ae. sharonensis* accession AEG-548-4 [https://www.genesys-pgr.org/a/ee4141c7-f78d-41a7-802f-84c42ab71c0c] have been deposited in the Lieberman-Okinow gene bank at the Institute for Cereal Crops Research (ICCR) at Tel Aviv University (https://en-lifesci.tau.ac.il/iccr). The D42 introgression parental line and its mutants are also available from ICCR at Tel Aviv University. The following public databases/datasets were used in this study: Chinese Spring reference genome[101], Gramene (http://www.gramene.org/), BLAST non-redundant protein sequence (https://blast.ncbi.nlm.nih.gov/Blast.cgi?PROGRAM=blastx&PAGE_TYPE=BlastSearch&LINK_LOC=blasthome). Source data are provided with this paper.

References

1. Khan, M. H., Bukhari, A., Dar, Z. A. & Rizvi, S. M. Status and strategies in breeding for rust resistance in wheat. *Agric. Sci.* **04**, 292–301 (2013).
2. Savary, S. et al. The global burden of pathogens and pests on major food crops. *Nat. Ecol. Evol.* **3**, 430–439 (2019).
3. Periyannan, S., Milne, R. J., Figueroa, M., Lagudah, E. S. & Dodds, P. N. An overview of genetic rust resistance: From broad to specific mechanisms. *PLoS Pathog.* **13**, 100638 (2017).
4. Dinh, H. X., Singh, D., Periyannan, S., Park, R. F. & Pourkheirandish, M. Molecular genetics of leaf rust resistance in wheat and barley. *Theor. Appl Genet.* **133**, 2035–2050 (2020).
5. Ali, S. et al. Origin, migration routes and worldwide population genetic structure of the wheat yellow rust pathogen Puccinia striiformis f.sp. tritici. *PLoS Pathog.* **10**, 1003903 (2014).
6. Hovmøller, M. S. et al. Replacement of the European wheat yellow rust population by new races from the centre of diversity in the near-Himalayan region. *Plant Pathol.* **65**, 402–411 (2016).

7. McDonald, B. A. & Stukenbrock, E. H. Rapid emergence of pathogens in agro-ecosystems: global threats to agricultural sustainability and food security. *Philos. Trans. R. Soc. B* **371**, 20160026 (2016).
8. Prank, M., Kenaley, S. C., Bergstrom, G. C., Acevedo, M. & Mahowald, N. M. Climate change impacts the spread potential of wheat stem rust, a significant crop disease. *Environ. Res. Lett.* **14**, 124053 (2019).
9. Hafeez, A. N. et al. Creation and judicious application of a wheat resistance gene atlas. *Mol. Plant* **14**, 1053–1070 (2021).
10. Cavalet-Giorsa, E. et al. Origin and evolution of the bread wheat D genome. *Nature* **633**, 848–855 (2024).
11. Knight, E. et al. Mapping the 'breaker' element of the gametocidal locus proximal to a block of sub-telomeric heterochromatin on the long arm of chromosome 4Ssh of Aegilops sharonensis. *Theor. Appl Genet.* **128**, 1049–1059 (2015).
12. Pont, C. et al. Tracing the ancestry of modern bread wheats. *Nat. Genet.* **51**, 905–911 (2019).
13. Tsujimoto, H. & Tsunewaki, K. Gametocidal genes in wheat and its relatives. I. Genetic analyses in common wheat of a gametocidal gene derived from Aegilops speltoides. *Can. J. Genet Cytol.* **26**, 78–84 (1984).
14. Sánchez-Martín, J. et al. Rapid gene isolation in barley and wheat by mutant chromosome sequencing. *Genome Biol.* **17**, 1–7 (2016).
15. Steuernagel, B. et al. Rapid cloning of disease-resistance genes in plants using mutagenesis and sequence capture. *Nat. Biotechnol.* **34**, 652–655 (2016).
16. Arora, S. et al. Resistance gene cloning from a wild crop relative by sequence capture and association genetics. *Nat. Biotechnol.* **37**, 139–143 (2019).
17. Gaurav, K. et al. Population genomic analysis of Aegilops tauschii identifies targets for bread wheat improvement. *Nat. Biotechnol.* **40**, 422–431 (2022).
18. Thind, A. K. et al. Rapid cloning of genes in hexaploid wheat using cultivar-specific long-range chromosome assembly. *Nat. Biotechnol.* **35**, 793–796 (2017).
19. Wang, Y. & Koo, D. An unusual tandem kinase fusion protein confers leaf rust resistance in wheat. *Nat. Genet.* **55**, 914–920 (2023).
20. Walkowiak, S. et al. Multiple wheat genomes reveal global variation in modern breeding. *Nature* **588**, 277–283 (2020).
21. Athiyannan, N., Aouini, L., Wang, Y. & Krattinger, S. G. Unconventional R proteins in the botanical tribe Triticeae. *Essays Biochem.* **66**, 561–569 (2022).
22. Mapuranga, J. et al. Harnessing genetic resistance to rusts in wheat and integrated rust management methods to develop more durable resistant cultivars. *Front. Plant Sci.* **13**, 951095 (2022).
23. Lolle, S., Stevens, D. & Coaker, G. Plant NLR-triggered immunity: from receptor activation to downstream signaling. *Curr. Opin. Immunol.* **62**, 99–105 (2020).
24. Yu, G. et al. Aegilops sharonensis genome-assisted identification of stem rust resistance gene Sr62. *Nat. Commun.* **13**, 1607 (2022).
25. Klymiuk, V., Coaker, G., Fahima, T. & Pozniak, C. J. Tandem protein kinases emerge as new regulators of plant immunity. *Mol. Plant Microbe Interact.* **34**, 1094–1102 (2021).
26. Li, H. et al. Wheat powdery mildew resistance gene Pm13 encodes a mixed lineage kinase domain-like protein. *Nat. Commun.* **15**, 2449 (2024).
27. Debernardi, J. M. et al. A GRF–GIF chimeric protein improves the regeneration efficiency of transgenic plants. *Nat. Biotechnol.* **38**, 1274–1279 (2020).
28. Hayta, S., Smedley, M. A., Clarke, M., Forner, M. & Harwood, W. A. An efficient agrobacterium-mediated transformation protocol for hexaploid and tetraploid wheat. *Curr. Protoc.* **1**, 58 (2021).
29. Wang, K. et al. The gene TaWOX5 overcomes genotype dependency in wheat genetic transformation. *Nat. Plants* **8**, 110–117 (2022).
30. Kishii, M. An update of recent use of Aegilops species in wheat breeding. *Front. Plant Sci.* **10**, 585 (2019).
31. Millet, E. Exploitation of Aegilops species of section Sitopsis for wheat improvement. *Isr. J. Plant Sci.* **55**, 277–287 (2007).
32. Scott, J. C., Manisterski, J., Sela, H., Ben-Yehuda, P. & Steffenson, B. J. Resistance of Aegilops species from Israel to widely virulent African and Israeli races of the wheat stem rust pathogen. *Plant Dis.* **98**, 1309–1320 (2014).
33. Anikster, Y., Manisterski, J., Long, D. L. & Leonard, K. J. Resistance to leaf rust, stripe rust, and stem rust in Aegilops spp. in Israel. *Plant Dis.* **89**, 303–308 (2005).
34. Huang, L. et al. Map-based cloning of leaf rust resistance gene Lr21 from the large and polyploid genome of bread wheat. *Genetics* **164**, 655–664 (2003).
35. Olivera, P. D., Kolmer, J. A., Anikster, Y. & Steffenson, B. J. Resistance of Sharon goatgrass (Aegilops sharonensis) to fungal diseases of wheat. *Plant Dis.* **91**, 942–950 (2007).
36. Millet, E. et al. Introgression of leaf rust and stripe rust resistance from Sharon goatgrass (Aegilops sharonensis Eig) into bread wheat (Triticum aestivum L.). *Genome* **57**, 309–316 (2014).
37. Khazan, S. et al. Reducing the size of an alien segment carrying leaf rust and stripe rust resistance in wheat. *BMC Plant Biol.* **20**, 1–13 (2020).
38. Steuernagel, B., Vrána, J., Karafiátová, M., Wulff, B. B. H. & Doležel, J. Rapid gene isolation using MutChromSeq. *Methods Mol. Biol.* **1659**, 231–243 (2017).
39. Ni, F. et al. Sequencing trait-associated mutations to clone wheat rust-resistance gene YrNAM. *Nat. Commun.* **14**, 4353 (2023).
40. Lee, W. S., Rudd, J. J. & Kanyuka, K. Virus induced gene silencing (VIGS) for functional analysis of wheat genes involved in Zymoseptoria tritici susceptibility and resistance. *Fungal Genet. Biol.* **79**, 84–88 (2015).
41. Sela, H. et al. Ancient diversity of splicing motifs and protein surfaces in the wild emmer wheat (Triticum dicoccoides) LR10 coiled-coil (CC) and leucine-rich repeat (LRR) domains. *Mol. Plant Pathol.* **13**, 276–287 (2012).
42. Sukarta, O. C. A., Slootweg, E. J. & Goverse, A. Structure-informed insights for NLR functioning in plant immunity. *Semin. Cell Biol.* **56**, 134–149 (2016).
43. Rhoads, A. & Au, K. F. PacBio sequencing and its applications. *Genom. Proteom. Bioinform.* **13**, 278–289 (2015).
44. Sedlazeck, F. J. et al. Accurate detection of complex structural variations using single-molecule sequencing. *Nat. Methods* **15**, 461–468 (2018).
45. Kiselev, K. V. et al. Influence of the 135 bp intron on stilbene synthase VaSTS11 transgene expression in cell cultures of grapevine and different plant generations of Arabidopsis thaliana. *Horticulturae* **9**, 513 (2023).
46. Meyberg, M. Selective staining of fungal hyphae in parasitic and symbiotic plant-fungus associations. *Histochemistry* **88**, 197–199 (1988).
47. Bailey, P. C. et al. Dominant integration locus drives continuous diversification of plant immune receptors with exogenous domain fusions. *Genome Biol.* **19**, 1–18 (2018).
48. Zhou, Y. et al. Allele mining for blast-resistance gene at Pi5 locus in rice. Plant. *Stress* **12**, 100465 (2024).
49. Akpinar, B. et al. The complete genome sequence of elite bread wheat cultivar, 'Sonmez'. *F1000Research* **11**, 614 (2022).
50. Sato, K. et al. Chromosome-scale genome assembly of the transformation-amenable common wheat cultivar 'Fielder. *DNA Res.* **28**, 8 (2021).

51. Zhou, Y. et al. Introgressing the Aegilops tauschii genome into wheat as a basis for cereal improvement. *Nat. Plants* **7**, 774–786 (2021).
52. Li, L. F. et al. Genome sequences of five Sitopsis species of Aegilops and the origin of polyploid wheat B subgenome. *Mol. Plant* **15**, 488–503 (2022).
53. Page, R. et al. Genome-wide association mapping of rust resistance in Aegilops longissima. *Front. Plant Sci.* **14**, 1196486 (2023).
54. Olivera, P. D., Anikster, Y. & Steffenson, B. J. Genetic diversity and population structure in Aegilops sharonensis. *Crop Sci.* **50**, 636–648 (2010).
55. Fukuoka, S. et al. Loss of function of a proline-containing protein confers durable disease resistance in rice. *Science* **325**, 998–1001 (2009).
56. Zhao, H. et al. The rice blast resistance gene Ptr encodes an atypical protein required for broad-spectrum disease resistance. *Nat. Commun.* **9**, 2039 (2018).
57. Krattinger, S. G. et al. A putative ABC transporter confers durable resistance to multiple fungal pathogens in wheat. *Science* **323**, 1360–1363 (2009).
58. Moore, J. W. et al. A recently evolved hexose transporter variant confers resistance to multiple pathogens in wheat. *Nat. Genet.* **47**, 1494–1498 (2015).
59. Narusaka, M., Hatakeyama, K., Shirasu, K. & Narusaka, Y. Arabidopsis dual resistance proteins, both RPS4 and RRS1, are required for resistance to bacterial wilt in transgenic Brassica crops. *Plant Signal Behav.* **9**, 29130 (2014).
60. Milligan, S. B. et al. The root knot nematode resistance gene Mi from tomato is a member of the leucine zipper, nucleotide binding, leucine-rich repeat family of plant genes. *Plant Cell* **10**, 1307–1319 (1998).
61. Rossi, M. et al. The nematode resistance gene Mi of tomato confers resistance against the potato aphid. *Proc. Natl Acad. Sci. USA* **95**, 9750–9754 (1998).
62. Nombela, G., Williamson, V. M. & Muñiz, M. The root-knot nematode resistance gene Mi-1.2 of tomato is responsible for resistance against the whitefly Bemisia tabaci. *Mol. Plant Microbe Interact.* **16**, 645–649 (2003).
63. Schultink, A., Qi, T., Lee, A., Steinbrenner, A. D. & Staskawicz, B. Roq1 mediates recognition of the Xanthomonas and Pseudomonas effector proteins XopQ and HopQ1. *Plant J.* **92**, 787–795 (2017).
64. Li, W., Deng, Y., Ning, Y., He, Z. & Wang, G. L. Exploiting broad-spectrum disease resistance in crops: from molecular dissection to breeding. *Annu. Rev. Plant Biol.* **71**, 575–603 (2020).
65. Brabham, H. J. et al. Barley MLA3 recognizes the host-specificity effector Pwl2 from Magnaporthe oryzae. *Plant Cell* **36**, 447–470 (2022).
66. Bettgenhaeuser, J. et al. The barley immune receptor Mla recognizes multiple pathogens and contributes to host range dynamics. *Nat. Commun.* **12**, 6915 (2021).
67. Brabham, H. J. et al. Rapid discovery of functional NLRs using the signature of high expression, high-throughput transformation, and large-scale phenotyping. *Cell*. Preprint at https://doi.org/10.2139/ssrn.4446759 (2023).
68. McIntosh, R. A. Nature of induced mutations affecting disease reaction in wheat. *Induced mutations against plant disease*. Vol. 9, 551–564 (International Atomic Energy Agency (IAEA), 1977).
69. Marais, G. F., McCallum, B. & Marais, A. S. Leaf rust and stripe rust resistance genes derived from Aegilops sharonensis. *Euphytica* **149**, 373–380 (2006).
70. Sánchez-Martín, J. & Keller, B. NLR immune receptors and diverse types of non-NLR proteins control race-specific resistance in Triticeae. *Curr. Opin. Plant Biol.* **62**, 102053 (2021).
71. Dinglasan, E., Periyannan, S. & Hickey, L. T. Harnessing adult-plant resistance genes to deploy durable disease resistance in crops. *Essays Biochem.* **66**, 571–580 (2022).
72. Ellis, J. G., Lagudah, E. S., Spielmeyer, W. & Dodds, P. N. The past, present and future of breeding rust resistant wheat. *Front. Plant Sci.* **5**, 641 (2014).
73. Chen, S., Zhang, W., Bolus, S., Rouse, M. N. & Dubcovsky, J. Identification and characterization of wheat stem rust resistance gene Sr21 effective against the Ug99 race group at high temperature. *PLoS Genet.* **14**, 1007287 (2018).
74. McIntosh, R. A. & Luig, N. H. Linkage of genes for reaction to Puccinia graminis f. sp. tritici and P. recondita in selkirk wheat and related cultivars. *Aust. J. Biol. Sci.* **26**, 1145–1152 (1973).
75. Zhang, W. et al. Identification and characterization of Sr13, a tetraploid wheat gene that confers resistance to the Ug99 stem rust race group. *Proc. Natl Acad. Sci. USA* **114**, 9483–9492 (2017).
76. Nakano, M. & Mukaihara, T. The type III effector RipB from Ralstonia solanacearum RS1000 acts as a major avirulence factor in Nicotiana benthamiana and other Nicotiana species. *Mol. Plant Pathol.* **20**, 1237–1251 (2019).
77. Faris, J. D. et al. A unique wheat disease resistance-like gene governs effector-triggered susceptibility to necrotrophic pathogens. *Proc. Natl Acad. Sci. USA* **107**, 13544–13549 (2010).
78. Avni, R. et al. Genome sequences of three Aegilops species of the section Sitopsis reveal phylogenetic relationships and provide resources for wheat improvement. *Plant J.* **110**, 179–192 (2022).
79. Kovaka, S., Ou, S., Jenike, K. M. & Schatz, M. C. Approaching complete genomes, transcriptomes and epi-omes with accurate long-read sequencing. *Nat. Methods* **20**, 12–16 (2023).
80. Long, D. & Kolmer, J. A North American system of nomenclature for Puccinia triticina. *Phytopathology* **79**, 525–529 (1986).
81. Roelfs, A. P. An international system of nomenclature for Puccinia graminis f. sp. tritici. *Phytopathology* **78**, 526–533 (1988).
82. Wan, A. & Chen, X. Virulence characterization of Puccinia striiformis f. sp. tritici using a new set of Yr single-gene line differentials in the United States in 2010. *Plant Dis.* **98**, 1534–1542 (2014).
83. Ben-David, R. et al. Differentiation among Blumeria graminis f. sp. tritici isolates originating from wild versus domesticated Triticum species in Israel. *Phytopathology* **106**, 861–870 (2016).
84. Huang, S., Steffenson, B. J., Sela, H. & Stinebaugh, K. Resistance of *Aegilops longissima* to the rusts of wheat. *Plant Dis.* **102**, 1124–1135 (2018).
85. Zadoks, J. C., Chang, T. T. & Konzak, C. F. A decimal code for the growth stages of cereals. *Weed Res.* **14**, 415–421 (1974).
86. Šimková, H., Číhalíková, J., Vrána, J., Lysák, M. & Doležel, J. Preparation of HMW DNA from plant nuclei and chromosomes isolated from root tips. *Biol. Plant* **46**, 369–373 (2003).
87. Giorgi, D. et al. FISHIS: fluorescence In Situ Hybridization in suspension and chromosome flow sorting made easy. *PLoS One* **8**, 57994 (2013).
88. Molnár, I. et al. Dissecting the U, M, S and C genomes of wild relatives of bread wheat (Aegilops spp.) into chromosomes and exploring their synteny with wheat. *Plant J.* **88**, 452–467 (2016).
89. Zhang, Y., Zhu, M. L. & Dai, S. L. Analysis of karyotype diversity of 40 Chinese chrysanthemum cultivars. *J. Syst. Evol.* **51**, 335–352 (2013).
90. Badaeva, E. D., Friebe, B. & Gill, B. S. Genome differentiation in Aegilops. 1. Distribution of highly repetitive DNA sequences on chromosomes of diploid species. *Genome* **39**, 293–306 (1996).
91. Šimková, H. et al. Coupling amplified DNA from flow-sorted chromosomes to high-density SNP mapping in barley. *BMC Genom.* **9**, 1–9 (2008).
92. Hummel, A. W. et al. Allele exchange at the EPSPS locus confers glyphosate tolerance in cassava. *Plant Biotechnol. J.* **16**, 1275–1282 (2018).

93. Zimin, A. V. et al. The MaSuRCA genome assembler. *Bioinformatics* **29**, 2669–2677 (2013).
94. Jackman, S. D. et al. ABySS 2.0: resource-efficient assembly of large genomes using a Bloom filter. *Genome Res.* **27**, 768–777 (2017).
95. Wicker, T., Matthews, D. E. & Keller, B. TREP: a database for Triticeae repetitive elements. *Trends Plant Sci.* **7**, 561–562 (2002).
96. Li, H. & Durbin, R. Fast and accurate short read alignment with Burrows-Wheeler transform. *Bioinformatics* **25**, 1754–1760 (2009).
97. Li, H. et al. The Sequence Alignment/Map format and SAMtools. *Bioinformatics* **25**, 2078–2079 (2009).
98. Robinson, J. T. et al. Integrative genomics viewer. *Nat. Biotechnol.* **29**, 24–26 (2011).
99. Wu, T. D. & Watanabe, C. K. GMAP: a genomic mapping and alignment program for mRNA and EST sequences. *Bioinformatics* **21**, 1859–1875 (2005).
100. Camacho, C. et al. BLAST+: architecture and applications. *BMC Bioinforma.* **10**, 1–9 (2009).
101. Appels, R. et al. Shifting the limits in wheat research and breeding using a fully annotated reference genome. *Science* **361**, 7191 (2018).
102. Doyle, J. J. & Doyle, J. L. A rapid DNA isolation procedure for small quantities of fresh leaf tissue. *Phytochem. Bull.* **19**, 11–15 (1987).
103. Sharma, D. et al. An efficient method for extracting next-generation sequencing quality RNA from liver tissue of recalcitrant animal species. *J. Cell Physiol.* **234**, 14405–14412 (2019).
104. Pfaffl, M. W. A new mathematical model for relative quantification in real-time RT–PCR. *Nucleic Acids Res.* **29**, 45 (2001).
105. Collier, R. et al. Accurate measurement of transgene copy number in crop plants using droplet digital PCR. *Plant J.* **90**, 1014–1025 (2017).
106. Giroux, M. J. & Morris, C. F. A glycine to serine change in puroindoline b is associated with wheat grain hardness and low levels of starch-surface friabilin. *Theor. Appl. Genet.* **95**, 857–864 (1997).
107. Li, Z., Hansen, J. L., Liu, Y., Zemetra, R. S. & Berger, P. H. Using real-time PCR to determine transgene copy number in wheat. *Plant Mol. Biol. Rep.* **22**, 179–188 (2004).
108. Bolger, A. M., Lohse, M. & Usadel, B. Trimmomatic: A flexible trimmer for Illumina sequence data. *Bioinformatics* **30**, 2114–2120 (2014).
109. Andrews, S. et al. *FastQC: a quality control tool for high throughput sequence data*. https://www.bioinformatics.babraham.ac.uk/projects/fastqc/ (2010).
110. Langmead, B. & Salzberg, S. L. Fast gapped-read alignment with Bowtie 2. *Nat. Methods* **9**, 357–359 (2012).
111. Dobin, A. et al. STAR: ultrafast universal RNA-seq aligner. *Bioinformatics* **29**, 15–21 (2013).
112. Li, B. & Dewey, C. N. RSEM: accurate transcript quantification from RNA-Seq data with or without a reference genome. *BMC Bioinforma.* **12**, 1–16 (2011).
113. RcoreTeam. R.: A Language and Environment for Statistical Computing (R Foundation for Statistical Computing, 2018).
114. Bateman, A. et al. UniProt: the universal protein knowledgebase in 2021. *Nucleic Acids Res.* **49**, 480–489 (2021).
115. Steuernagel, B. et al. The NLR-annotator tool enables annotation of the intracellular immune receptor repertoire. *Plant Physiol.* **183**, 468–482 (2020).
116. Bailey, T. L. & Gribskov, M. Combining evidence using p-values: application to sequence homology searches. *Bioinformatics* **14**, 48–54 (1998).
117. Martin, E. C. et al. NLRscape: an atlas of plant NLR proteins. *Nucleic Acids Res.* **51**, 1470–1482 (2022).
118. Kelley, L. A., Mezulis, S., Yates, C. M., Wass, M. N. & Sternberg, M. J. E. Europe PMC Funders Group The Phyre2 web portal for protein modelling, prediction and analysis. *Nat. Protoc.* **10**, 845–858 (2015).
119. Jumper, J. et al. Highly accurate protein structure prediction with AlphaFold. *Nature* **596**, 583–589 (2021).
120. van Kempen, M. et al. Fast and accurate protein structure search with Foldseek. *Nat. Biotechnol.* **42**, 243–246 (2024).
121. De Beukelaer, H., Davenport, G. F. & Fack, V. Core Hunter 3: flexible core subset selection. *BMC Bioinforma.* **19**, 1–12 (2018).
122. Edgar, R. C. M. U. S. C. L. E. Multiple sequence alignment with high accuracy and high throughput. *Nucleic Acids Res.* **32**, 1792–1797 (2004).
123. Martin, D. P. et al. RDP5: a computer program for analyzing recombination in, and removing signals of recombination from, nucleotide sequence datasets. *Virus Evol.* **7**, 087 (2021).
124. Yuan, C. et al. A high throughput barley stripe mosaic virus vector for virus induced gene silencing in monocots and dicots. *PLoS One* **6**, 26468 (2011).
125. Zhang, R. et al. Generation of herbicide tolerance traits and a new selectable marker in wheat using base editing. *Nat. Plants* **5**, 480–485 (2019).
126. Liu, Z. & Friesen, T. DAB staining and visualization of hydrogen peroxide in wheat leaves. *Bio-protocol* **2**, 309 (2012).
127. Wenger, A. M. et al. Accurate circular consensus long-read sequencing improves variant detection and assembly of a human genome. *Nat. Biotechnol.* **37**, 1155–1162 (2019).
128. Eid, J. et al. Real-time DNA sequencing from single polymerase molecules. *Science* **323**, 133–138 (2009).
129. Marone, M. P., Singh, H. C., Pozniak, C. J. & Mascher, M. A technical guide to TRITEX, a computational pipeline for chromosome-scale sequence assembly of plant genomes. *Plant Methods* **18**, 128 (2022).

Acknowledgements

The research was supported by BARD grant # IS-5087-18 R to A.M-D., A.S., and G.M., The Lieberman Family and the JNF Australia donations to A.S., and by the Lieberman-Okinow Endowment at Tel Aviv University to the Institute for Cereal Crops Research. D.S. was supported by PBC fellowship of the Council for Higher Education of Israel; M.J.M. received funding from the 2Blades Foundation, Japan Tobacco Inc., KANEKA CORPORATION, the United Kingdom Research and Innovation-Biotechnology and Biological Sciences Research Council Institute Strategic Programme (UKRI-BBSRC ISP; grant no. BBS/E/J/000PR9795), the Gatsby Charitable Foundation, and United States Department of Agriculture-Agricultural Research Service CRIS #5062-21220-025-000D; BBHW received funding from the 2Blades Foundation, and the UKRI-BBSRC ISP (grant no. BBS/E/J/000PR9780); J.D. received funding from ERDF project 'Plants as a tool for sustainable global development', No. CZ.02.1.01/0.0/0.0/16_019/0000827. We thank Zdeňka Dubská, Romana Šperková, and Jitka Weiserová for the preparation of chromosome samples for flow cytometry. We thank Cathy Melamed-Bessudo for providing the modified CTAB protocol (PacBio-grade sequencing) and Yamit Bar-Lev for assistance with the DNA extraction process.

Author contributions

Generated the *Ae. longissima* population: B.J.S., H.S., M.R.; Generated the *Ae. sharonensis* EMS mutants: E.M. S.H-K., A.M-D.; Generated the *Ae. sharonensis* population: O.S., O.Maatuk.; Participated in the phenotyping: S.E., H.S., J.M., P.B-Y., M.R., A.M-D., O.Matny., O.S., B.J.S.; Performed chromosome flow sorting and amplification: I.M., K.H., M.S., J.D.; Chromosome assembly: R.A., M.M.; AgRenSeq analysis: R.A., H.S.; DNA and RNA extraction: D.S., O.Maatuk, S.E., M.R-P., R.K., A.M-D., A.S-C., G.Y.; Mut transcriptomics analysis: J.G-G., G.J.M.; Bioinformatic analyses, annotation and localization of *Yr87/Lr85*: U.L., A.M-D., R.A.; Analysis of the *Ae. sharonensis* gene: G.B., G.J.M.; Isolation and subcloning of *Yr87/Lr85:* D.S.; Developed the binary vectors: D.S., R.K., A.S-C., A.M-D.; Produced transgenic wheat plants: R.K., A.S-C., DS; Performed rust, ROS and callose staining: A.M-D., T.E., Y.L.; Generated and performed VIGS: D.S.; Quantitative real-time PCR: D.S.; Transgenic copy number assay: D.S., A.M-D., M.R-P.; Performed phylogenetics analyses: M.J.M.,

M.R-P., H.S., R.A., U.L., H.J-B., M.M.; Performed protein structure analysis: M.J.M., O.S.; Provided germplasm, rust cultures or scientific support and advice: B.B.H.W., Y.A., J.M., E.M., B.J.S.; Conceived study: A.S., A.M-D., G.J.M.; Drafted manuscript: A.S., A.M.D., D.S., G.J.M., B.B.H.W, M.J.M.

Competing interests

The authors declare the following competing interests: D.S., R.A., R.K, E.M., A.M-D., and A.S. are inventors on the US patent application 63/250,413 filed by Ramot (Tel Aviv University) and relating to the use of *Yr87/Lr85* for leaf and stripe rust resistance in transgenic wheat. All other authors claim no competing interests.

Additional information

Supplementary information The online version contains supplementary material available at https://doi.org/10.1038/s41467-024-54068-6.

Correspondence and requests for materials should be addressed to Gary Muehlbauer, Anna Minz-Dub or Amir Sharon.

Peer review information *Nature Communications* thanks the anonymous reviewers for their contribution to the peer review of this work. A peer review file is available.

[1]The Institute for Cereal Crops Research, Tel Aviv University, Tel Aviv, Israel. [2]School of Plant Sciences and Food Security, Tel Aviv University, Tel Aviv, Israel. [3]Leibniz Institute of Plant Genetics and Crop Plant Research (IPK) Gatersleben, Seeland, Germany. [4]Department of Agronomy and Plant Genetics, University of Minnesota, St. Paul, MN, USA. [5]Departamento de Biología Molecular, Universidad de León, León, Spain. [6]Institute of Evolution, University of Haifa, Haifa, Israel. [7]Institute of Experimental Botany of the Czech Academy of Sciences, Centre of Plant Structural and Functional Genomics, Olomouc, Czechia. [8]Field Crops Research Institute, Agricultural Research Centre, Cairo, Egypt. [9]Department of Plant Pathology, University of Minnesota, St. Paul, MN, USA. [10]German Centre for Integrative Biodiversity Research (iDiv) Halle-Jena-Leipzig, Leipzig, Germany. [11]The Sainsbury Laboratory, Norwich Research Park, Norwich, UK. [12]2Blades, Evanston, IL, USA. [13]USDA-ARS, Cereal Disease Laboratory, University of Minnesota, St. Paul, MN, USA. [14]John Innes Centre, Norwich Research Park, Norwich, UK. [15]Plant Science Program, Biological and Environmental Science and Engineering Division (BESE), King Abdullah University of Science and Technology (KAUST), Thuwal, Saudi Arabia. [16]Present address: USDA-ARS, Western Regional Research Center, Crop Improvement and Genetics Research Unit, Albany, CA, USA. [17]Present address: Agricultural Institute, Centre for Agricultural Research, ELKH, Martonvásár, Hungary. [18]Deceased: Yehoshua Anikster. ✉e-mail: muehl003@umn.edu; annamin1@tauex.tau.ac.il; amirsh@tauex.tau.ac.il